JOURNAL OF PHARMACEUTICAL SCIENCES

NOVEMBER 1983
VOLUME 72 NUMBER 11

RESEARCH ARTICLES

# Physiologically Based Pharmacokinetic Model for β-Lactam Antibiotics I: Tissue Distribution and Elimination in Rats

AKIRA TSUJI *x, TAKAYOSHI YOSHIKAWA *, KAZUNORI NISHIDE *, HIDEMI MINAMI *, MOTONOBU KIMURA *, EMI NAKASHIMA *, TETSUYA TERASAKI *, ETSUKO MIYAMOTO *¶, CHARLES H. NIGHTINGALE §, and TSUKINAKA YAMANA ‡

Received April 5, 1982, from the *Faculty of Pharmaceutical Sciences and ‡Hospital Pharmacy, Kanazawa University, Kanazawa 920, Japan and §Hartford Hospital, Hartford, CT 06115 and University of Connecticut, School of Pharmacy, Storrs, CT 06268. Accepted for publication September 2, 1982. ¶Present address: School of Pharmacy, Hokuriku University, Kanazawa 920-11, Japan.

**Abstract** □ The disposition characteristics of β-lactam antibiotics in rats were investigated, and a physiologically based pharmacokinetic model capable of predicting the tissue distribution and elimination kinetics of these drugs was developed. Protein-binding parameters in rat serum were determined by equilibrium dialysis. Linear binding was found for penicillin G, methicillin, dicloxacillin, and ampicillin; however, nonlinear binding was observed for penicillin V and cefazolin. After intravenous bolus dosing, cefazolin was recovered almost completely in urine and bile, while for the penicillins, penicilloic acid was found to be the major metabolite. Biliary excretion of cefazolin followed Michaelis-Menten kinetics, and no significant inhibition of urinary secretion was observed after probenecid administration. The renal clearance of unbound drug was 0.82 ml/min with a reabsorption ratio (R) of 0.22. Tubular secretion was inhibited for the penicillins by probenecid plasma concentrations of 50 μg/ml, resulting in an R-value of 0.32. Erythrocyte uptake, serum protein binding, and tissue-to-plasma partition coefficient ($K_p$) were measured. Theoretical $K_p$ values were calculated and found to be in good agreement with the $K_p$ values for three of the antibiotics. Plasma and tissue concentrations (lung, heart, muscle, skin, gut, bone, liver, and kidney) were measured as a function of time at various doses for inulin and cefazolin in rats after an intravenous bolus dose, and were found to be in reasonable agreement with concentrations predicted by the model. These correlations demonstrate that the proposed model can accurately describe the plasma and tissue contributions of inulin and cefazolin in the rat and suggest that this model could have utility in predicting drug distribution in humans.

**Keyphrases** □ β-Lactam antibiotics—protein binding and metabolism, rats, pharmacokinetics, physiologically based model □ Pharmacokinetics—β-lactam antibiotics, protein binding and metabolism in rats, physiologically based model □ Metabolism—β-lactam antibiotics in rats, pharmacokinetics, physiologically based model

Serum or plasma levels of antibiotics are often used as indices of pharmacological efficacy. However, since bacterial infections are generally localized in the extravascular space, it is important to know the antibiotic concentration in the interstitial fluid. Numerous pharmacokinetic studies on penicillins and cephalosporins have been published (1–6); however, few compare kinetically the levels of these antibiotics in plasma and tissues. Physiologically based pharmacokinetic models (7–12) have been developed using data obtained from animals such as tissue binding or tissue-to-plasma partition coefficients ($K_p$). Some of these studies have been used successfully to predict both plasma and tissue levels in humans (7–9, 11). Recently, Greene *et al.* (13) reported that using serum protein binding and renal clearance data, the novel physiological pharmacokinetics of cephalosporins could be adapted to predict plasma concentration–time profiles after bolus intravenous injections in humans.

This study describes the metabolism and tissue binding behavior of several β-lactam antibiotics in rats, establishes a mathematical model for the interpretation of tissue distribution and elimination kinetics of these antibiotics, and describes the use of inulin as a model drug for verification of the present model.

## EXPERIMENTAL

**Materials**—Penicillin G potassium (1595 U/mg)[1], methicillin sodium (843 μg/mg)[2], penicillin V potassium (1490 U/mg)[1], propicillin potassium (888 μg/mg)[3], dicloxacillin sodium (884 μg/mg)[1], ampicillin sodium (959 μg/mg)[3], 6-aminopenicillanic acid (97.6% pure)[1], cefazolin sodium (945

[1] Meiji Seika Kaisha, Tokyo, Japan.
[2] Banyu Pharmaceutical Co., Tokyo, Japan.
[3] Takeda Chemical Industries, Osaka, Japan.

0022-3549/83/1100-1239$01.00/0

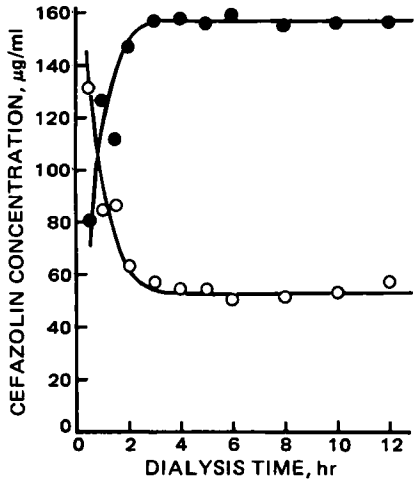


**Figure 1**—*Cefazolin concentrations in buffer (○) and rat serum (●) compartments at 37° during the protein binding experiment. The initial concentration of cefazolin in the buffer compartment was 200 μg/ml.*

μg/mg)[4], *and indocyanine green*[5] were used as received. [$^{14}$C]Cefazolin[4] with a specific activity of 2.04 μCi/mg was supplied, and [$^{14}$C]inulin (2.4 μCi/mg) was purchased from a commercial source[6]. Unless otherwise specified, the radiolabeled drug was used in conjunction with a cold carrier.

Solutions of the penicilloic acids of dicloxacillin, propicillin, penicillin V, ampicillin, and 6-aminopenicillanic acid were prepared according to the method of Schwartz and Delduce (14). All other chemicals were reagent grade and were used without further purification.

**Animals**—Male albino Wistar rats, weighing ~240 g, and a 9-kg beagle dog were fasted for 20 hr prior to the experiment, with free access to water. The rats were anesthetized with urethane (1.3 g/kg ip) ~1 hr prior to surgery. The dog was anesthetized with sodium pentobarbital[7] administered intravenously at a dose of 25 mg/kg.

**Intravenous Bolus Injection**—The ureters and bile ducts of rats were catheterized with polyethylene tubing[8], and the drugs were injected (over 5 sec) through the femoral vein. The β-lactam antibiotics or inulin were dissolved in 0.5 ml of normal saline. For the plasma and tissue concentration studies, blood samples (~0.2 ml) were withdrawn from the jugular vein at designated times after drug administration and collected in heparinized tubes. The blood was centrifuged at 3000 rpm, and plasma

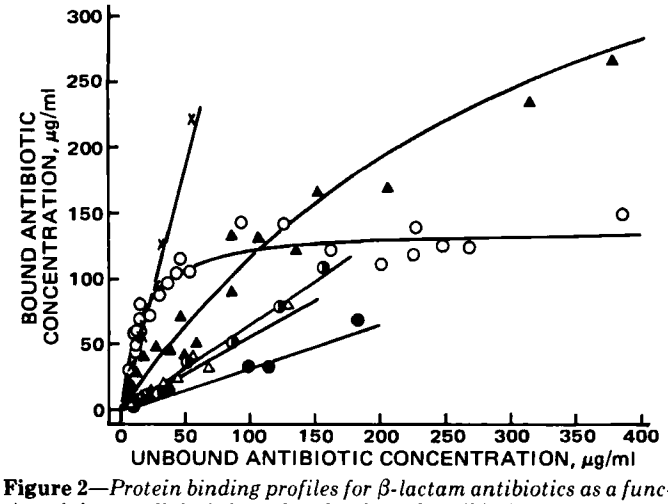


**Figure 2**—*Protein binding profiles for β-lactam antibiotics as a function of the postdialysis bound and unbound antibiotic concentrations at 37°. The points represent the experimental values, and the solid lines were generated from Eq. 1 or Eq. 2; the binding parameters are listed in Table I. Key: (●) methicillin; (△) penicillin G; (◑) ampicillin; (○) cefazolin; (▲) penicillin V; (X) dicloxacillin.*

[4] Fujisawa Pharmaceutical Co., Osaka, Japan.
[5] Daiichi Seiyaku Co., Tokyo, Japan.
[6] New England Nuclear Co., Boston, Mass.
[7] Nembutal; Dainihon Pharmaceutical Co., Osaka, Japan.
[8] Type PE-10; Clay Adams, Becton Dickinson, Co., Parsippany, N.J.

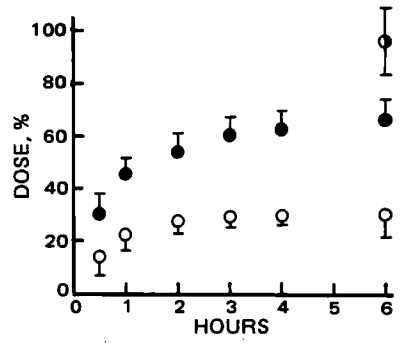


**Figure 3**—*Time courses of the percent of cefazolin recovered in bile (○) and urine (●) after a 100-mg/kg iv bolus dose to rats. Each point represents the mean of four rats, the vertical bars representing the standard deviations. Total recovery (◑), as the intact cefazolin 6 hr after the administration, was 95.7 ± 13.0%.*

separated. The total blood volume taken from any rat in a single experiment was ≤1.6 ml.

For tissue sampling, the rats were sacrificed, and the lung, heart, skeletal muscle, bone, gut (from duodenum to the cecum), liver, and kidney were quickly excised, rinsed with ice-cold saline, blotted dry, and weighed. These tissues were homogenized with a two- to fivefold excess of isotonic phosphate buffer (pH 7.4) in a polytef homogenizer. The entire skin was stripped from the rat carcass. Sections of the skin from the flank regions were sampled and cut into small pieces. Bone samples were taken from the femoral and foreleg portions and crushed. The chips of skin and bone were weighed and extracted with isotonic phosphate buffer (pH 7.4) by shaking for 4 hr. The fluids were then centrifuged at 3000 rpm for 10 min, and the supernatant was removed for microbiological assay of cefazolin and for the colorimetric assay of inulin.

In the experiments using radioactive drugs, the rats were injected with a 10- to 200-mg/kg dose of cefazolin or a 20-mg/kg dose of inulin, each of which contained radiolabeled drug. The excised tissue samples were rinsed with ice-cold saline and blotted dry. One-half of the dry tissue was used for analysis.

**Determination of Hepatic Blood Flow**—The hepatic blood flow of rats under urethane or ether anesthesia was estimated using the method of Yokota *et al.* (15). A priming dose of indocyanine green was injected into the femoral vein of the rat and immediately followed by a constant infusion[9] of the dye into the opposite femoral vein at a rate of 13–27 μg/min, yielding a steady-state plasma level of ~10 μg/ml. Three blood samples (0.2 ml each) were simultaneously withdrawn from the hepatic vein and femoral artery every 10 min starting 60 min after the initiation of the dye injection. The plasma was separated by centrifugation and stored at 4° until assayed. Aliquots (50–100 μl) of the plasma were diluted 10- to 20-fold with distilled water and quantified by measurement of the absorbance at 800 nm[10]. Hematocrits (Hct, %) were measured[11] using the first and last arterial and hepatic venous blood samples, and averaged. The hepatic plasma and blood flows were calculated with the equation of Bradley *et al.* (16).

**Determination of Tissue-to-Plasma Partition Coefficients**—The equilibrium tissue-to-plasma concentration ratios, $K_p$, of penicillin V, dicloxacillin, cefazolin, and [$^{14}$C]inulin were obtained experimentally for each of the tissues used in the pharmacokinetic model. Solutions of the penicillins, cefazolin with or without added [$^{14}$C]cefazolin, and inulin containing [$^{14}$C]inulin prepared with saline were infused[9] at a rate of 0.5 ml/hr through the femoral vein of rats. Based on the preliminary experimental data collected after intravenous bolus injection of each drug, a priming dose was administered to quickly attain a steady-state condition.

Blood samples were withdrawn periodically through the jugular vein. After 2 or 3 hr of infusion, blood samples from the femoral artery, renal vein, and hepatic vein were taken. The animals were sacrificed immediately by exsanguination *via* the carotid artery. Tissue samples taken at the steady-state plasma level were prepared in the same manner as described above for bolus-dose experiments.

The distribution of antibiotics into erythrocytes and bone marrow were studied under the conditions described above. In addition, a beagle dog was infused with cefazolin at a rate of 180 mg/hr, without a priming dose,

[9] Infusion pump model KN; Natsume Seisakusho Co., Tokyo, Japan.
[10] Double-beam spectrophotometer, UV-200; Shimadzu, Kyoto, Japan.
[11] Hematocrit MC-200; Hitachi Koki Co., Tokyo, Japan.

**Table I—Binding Parameters [a] of β-Lactam Antibiotics with Rat Serum Protein**

| β-Lactam Antibiotic | $n$ [b] | $10^{-4} K_B$ [b], $M^{-1}$ | $10^{-4} K_{B,app}$ [c], $M^{-1}$ |
|---|---|---|---|
| Penicillin G | — | — | 1.132 ± 0.048 |
| Penicillin V | 2.78 ± 0.26 | 0.109 ± 0.014 | — |
| Methicillin | — | — | 0.656 ± 0.070 |
| Ampicillin | — | — | 1.322 ± 0.048 |
| Dicloxacillin | — | — | 7.434 ± 0.448 |
| Cefazolin | 0.63 ± 0.03 | 2.980 ± 0.479 | — |

[a] The binding parameters were determined by the equilibrium dialysis method at 37°. An albumin concentration of $5.00 \times 10^{-4}$ $M$ was used for calculation. [b] Defined by Eq. 1. [c] Defined by Eq. 2.

over a 10-hr period. After achievement of steady-state levels, aliquots of blood were withdrawn periodically through a cannula inserted into the saphenous vein of the dog. Bone marrow fluids were withdrawn periodically from a portion of femoral bone using the usual puncture technique. The hematocrits of the blood samples were determined[11]. Antibiotic concentrations of the whole blood and whole bone marrow were determined after hemolysis with an equivalent volume of distilled water. The results were used to estimate the partition coefficients of these antibiotics between plasma and erythrocytes and between plasma and bone marrow.

**Determination of Renal and Hepatic Clearances**—Intravenous infusions were performed to measure the renal and hepatic clearances of penicillin G or cefazolin at steady state in rats. In the renal clearance measurements, the femoral artery, femoral vein, left renal vein, and ureters were cannulated. Antibiotic solutions containing inulin to estimate the glomerular filtration rate (GFR) were prepared with 3% mannitol and infused[9] at a rate of 3.7 ml/hr through the femoral vein using a priming dose for each drug. After constant urine flow and steady-state levels of the antibiotic and inulin were achieved, urine was collected over 30-min intervals and blood was withdrawn through the femoral artery and renal vein at the midpoint of the urine collection period. The renal excretion rate ($dX_u/dt$) was calculated from $dX_u/dt = C_u UF$, where $C_u$ and UF indicate the urine concentration of drug and urine flow in ml/min, respectively.

The inhibitory effect of probenecid on the tubular secretion of penicillin G and cefazolin were examined as follows. Probenecid was dissolved in aqueous sodium hydroxide and then neutralized with hydrochloric acid. A 3% mannitol solution containing penicillin G, cefazolin, or inulin, and probenecid was infused at a rate of 3.7 ml/hr. In each experiment, the steady-state plasma concentration of probenecid was assayed.

The procedure used to measure the hepatic clearance of cefazolin, was essentially the same as that described for determining hepatic plasma flow. At steady state, the total plasma concentration (bound and unbound) of cefazolin in the femoral artery, hepatic vein, and bile were determined by microbiological assay.

**Determination of Serum Protein Binding**—Acrylic resin plates with four compartments of 5 mm depth and 25 mm diameter were used for the dialysis studies. Two plates were joined tightly, holding a cellulose membrane[12] between them. An 0.8-ml aliquots of rat serum was put into one compartment and, unless otherwise specified, 0.8 ml of pH 7.4 isotonic phosphate buffer containing an appropriate concentration of antibiotic was put into the other compartment. The plates were incubated for 6 hr at 37°. After appropriate dilution of equilibrated samples with the isotonic phosphate buffer, the antibiotic concentrations in both compartments were measured by microbiological assay. The concentration of the antibiotic bound to serum protein was obtained by subtracting the concentration of unbound drug from the total drug concentration. When the effect of the buffer component on the binding ratio was investigated, the following solutions were used instead of isotonic phosphate buffer: Tris-hydrochloride buffer (pH 7.4), 0.067 $M$ phosphate buffer (pH 7.4), and protein-free rat serum obtained by ultrafiltration[13] of pooled serum.

**Paper Chromatography**—Paper chromatography was conducted in a cold room according to the method of Thomas (17). The developing solvent was $n$-butyl alcohol–pyridine–water (1:1:1). A portion of the urine or bile sample was treated with 1 $N$ NaOH for 20 min at room temperature followed by neutralization with 1 $N$ HCl, and 10 μl was spotted on the paper[14]. Ten microliters of the untreated portion was spotted directly on the paper. The chromatograms were visualized by spraying with 1% starch in acetic acid–0.1 $N$ $I_2$–4% KI (50:3:1). For detection of intact penicillin V, the paper was sprayed with 0.1 $N$ NaOH and after 20 min sprayed with 0.1 $N$ HCl. Standard samples of each penicillin and penicilloic acid were prepared using normal urine and bile and were chromatographed similarly as a reference marker.

**Table II—Urinary and Biliary Recoveries (Percent of Dose) of Penicillin V and Its Metabolites after Intravenous Administration in Rats [a]**

| Compound | Urine, % | Bile, % | Total, % |
|---|---|---|---|
| Penicillin V | 13.8 ± 6.6 | 29.5 ± 3.1 | 43.3 ± 7.3 |
| Phenoxymethylpenicilloic acid | 17.1 ± 2.2 | 18.7 ± 1.0 | 35.8 ± 2.4 |
| 6-Aminopenicillanic acid and its penicilloic acid | 6.9 ± 2.8 | 15.1 ± 2.0 | 22.0 ± 3.4 |
| Total | | | 101.1 ± 8.4 |

[a] The urine and bile collection periods were 0–9 hr and the dose was 100 mg/kg. Each point represents the mean of three rats ± $SD$.

**Analytical Procedures**—*Microbiological Assay*—Plasma, urine, bile, and tissue samples from rats administered β-lactam antibiotics were assayed (unless otherwise specified) by the microbiological paper disk diffusion method using *Sarcina lutea*[15], *Staphylococcus aureus*[16], or *Bacillus subtilis*[17] as the test organism. In the determination of drug distribution into erythrocytes, blood samples used for plasma quantification were hemolyzed with an equal volume of distilled water and analyzed. Calculation of the antibiotic concentration was made from standard curves prepared using pooled blood, urine, bile, and the corresponding tissue homogenates. The accuracy of the microbiological assay was ±5%.

*Spectrofluorometric Assay*—Spectrofluorometric methods were utilized for simultaneous analysis of a penicillin and the penicilloic acid metabolite in whole blood, urine, and bile. The blood was hemolyzed with an equal volume of distilled water. The analytical method employed for samples taken after intravenous administration of penicillin V, propicillin, or dicloxacillin was based on the formation of a fluorescent Schiff-base resulting from the reaction between penicilloaldehyde and 0.1% 5-dimethylaminonaphthalene-1-sulfonylhydrazine. After acylation with phenoxyacetic anhydride at pH 9.0, 6-aminopenicillanic acid and its cleaved β-lactam ring product were assayed as described previously[18] (18). The method of Miyazaki *et al.* (19) was used for quantification of ampicillin. The accuracy of the fluorometry assay was ±4%.

*Radiochemical Assay*—The radioactivity of [$^{14}$C]cefazolin and [$^{14}$C]inulin in plasma was determined by direct liquid scintillation counting[19]. Triplicate 50–250-μl aliquots of plasma were added to glass counting vials containing 10 ml of dioxane-based scintillation fluid. Quenching was corrected by the external standard method. Tissue samples after intravenous bolus dosing or constant infusion were oxidized[20] to $^{14}CO_2$, and radioactivity was determined by liquid scintillation counting[19].

*Determination of Inulin*—The method used for the determination of inulin in plasma, urine, and lung tissue was a modified form of the colorimetric assay developed by Waugh (20). Reagents and standard solutions of inulin were prepared as described previously (20). Samples of plasma (0.1 ml), 0.3 ml of distilled water, and 0.1 ml of zinc sulfate reagent were added to centrifuge tubes, followed by the addition (with continuous agitation) of 0.1 ml of 0.5 $N$ NaOH. After centrifugation at 3000 rpm for 10 min, the supernatant was removed for analysis. Urine was assayed by adding 0.5 ml of zinc sulfate reagent and 0.5 ml of 0.5 $N$ NaOH to 1.0 ml of urine, yielding a protein-free supernatant. For tissue sample assay, the tissue was cut into small pieces. The chips were weighed and extracted with saline by shaking for 4 hr. The fluids were then centrifuged at 3000 rpm for 10 min, and the supernatant was analyzed.

Aliquots (0.2 ml) of the supernatant from plasma, urine, or tissue samples were placed in a test tube, 0.2 ml of 1.8 $N$ NaOH was added, and

[12] VisKing; Ethyl Corp.
[13] Amicon MMC, Lexington, Mass.
[14] Toyo Roshi No. 50, 2 × 40 cm; Toyo Roshi Co., Tokyo, Japan.
[15] IFO 12708; Institute for Fermentation, Osaka, Japan. The strain was derived from ATCC 9341.
[16] IFO 12732; Institute for Fermentation, Osaka, Japan. The strain was derived from ATCC 6538P.
[17] IFO 3134; Institute for Fermentation, Osaka, Japan. The strain was derived from ATCC 6633.
[18] In a previous paper (18), the concentration of 5-dimethylaminonaphthalene-1-sulfonylhydrazine reagent was erroneously referred to as 10%. The correct concentration is 0.1%. The full paper on the detailed procedure and the results are in preparation.
[19] Model LSC-671; Aloka Co., Tokyo, Japan.
[20] Sample oxidizer, Model 306; Packard Instruments, Downers Grove, Ill.

**Table III—Urinary and Biliary Recoveries (Percent of Dose) of Penicillins and Their Penicilloic Acids after Intravenous Administration in Rats [a]**

| Penicillin | Intact Penicillin, % | | | Penicilloic Acid, % | | |
|---|---|---|---|---|---|---|
| | Urine | Bile | Total | Urine | Bile | Total |
| Penicillin G [b] | 30.0 ± 13.8 | 25.7 ± 3.6 | 55.7 ± 14.3 | 3.7 ± 1.0 | 12.9 ± 2.9 | 16.6 ± 3.1 |
| Propicillin | 19.1 ± 11.1 | 24.2 ± 2.4 | 43.3 ± 11.4 | 4.4 ± 1.3 | 21.0 ± 2.0 | 25.4 ± 2.4 |
| Dicloxacillin | 9.6 ± 6.0 | 14.4 ± 7.1 | 24.0 ± 9.3 | 5.5 ± 3.1 | 24.4 ± 3.4 | 29.9 ± 4.6 |
| Ampicillin | 34.9 ± 13.2 | 19.5 ± 2.3 | 54.4 ± 13.4 | 3.2 ± 1.4 | 9.9 ± 4.1 | 13.1 ± 4.3 |

[a] The urine and bile collection periods were 0–3 hr; the dose was 100 mg/kg. Each point represents the mean of three rats ± *SD*. [b] The urine and bile collection periods were 0–24 hr; the dose was 100 mg/kg. Each point represents the mean of eight rats ± *SD*.

the mixture was heated at 100° for 10 min. The mixture was cooled and 3 ml of 70% (v/v) $H_2SO_4$ and 0.3 ml of cysteine–tryptophan reagent was added. After heating at 50° for 25 min, the solution was cooled to room temperature and the color was evaluated against a blank[11] at 515 nm.

*Determination of Probenecid*—Concentrations of probenecid in plasma and urine were determined by a high-performance liquid chromatographic (HPLC) assay (21). Samples were prepared as described previously (21), but the chromatographic conditions were modified slightly. A reverse-phase column[21] (25 cm × 4.6-mm i.d.), packed in this laboratory, was used in conjunction with a chromatograph[22] equipped with a variable-wavelength detector[23]. The mobile phase was acetonitrile–0.014 *M* pH 6.0 phosphate buffer (3:7). The column and solvent were kept at ambient temperature. A flow rate of 2.5 ml/min was used, yielding an operating pressure of 110 kg/cm$^2$. The spectrophotometric detector had an 8-μl flow cell and was operated at 254 nm; the injection volume was 50 μl. Complete peak resolution was obtained with a retention time of 4 min. Peak heights were used for quantification; standard curves were generated by blank plasma and urine samples spiked with varying amounts of probenecid as described previously (21).

**Data Analysis**—The data were analyzed using a digital computer[24]. The program used for the physiologically based pharmacokinetic models was designed in-house by incorporating the NUMINT program, a subroutine in NONLIN (22).

## RESULTS

**Serum Protein Binding**—Cefazolin diffused rapidly from the buffer compartment into the serum compartment (Fig. 1). Equilibrium was established within 4 hr and was maintained for the 12-hr duration of the experiment. The effect of buffer components on the binding behavior of cefazolin was also examined. The percentage of cefazolin bound at a total concentration of 70 μg/ml was determined to be 85.6 ± 3.4, 86.8 ± 3.6, 88.3 ± 1.8, and 85.1 ± 3.0 in isotonic phosphate buffer (pH 7.4), 0.067 *M* phosphate buffer (pH 7.4), Tris-hydrochloride buffer, and protein-free rat serum, respectively. These differences were not statistically significant.

Figure 2 illustrates the protein binding profiles for each of the studied β-lactam antibiotics as a function of the postdialysis antibiotic concentration. The protein binding behavior varied among antibiotics. Nonlinear protein binding was observed for cefazolin and penicillin V, whereas apparent linear binding was found for penicillin G, methicillin, dicloxacillin, and ampicillin. Assuming that albumin is the sole binding protein for β-lactam antibiotics, then:

$$C_B = \frac{nPK_BC_F}{1 + K_BC_F} \qquad \text{(Eq. 1)}$$

where $C_B$ and $C_F$ are the concentrations of antibiotic bound and unbound with serum protein, $n$ is the number of binding sites on the albumin molecule, $K_B$ is the affinity constant for albumin, and $P$ is the albumin concentration (mol. wt. 69,000) in serum. (Measured values for $P$ averaged $5.0 \times 10^{-4}$ *M*.) The nonlinear least-squares regression computer program, NONLIN, was used to fit the data to Eq. 1. In the case of linear binding, simplification of Eq. 1 yields:

$$C_B = K_{B,app}PC_F \qquad \text{(Eq. 2)}$$

where $K_{B,app}$ is the apparent affinity constant for albumin. The binding parameters are presented in Table I.

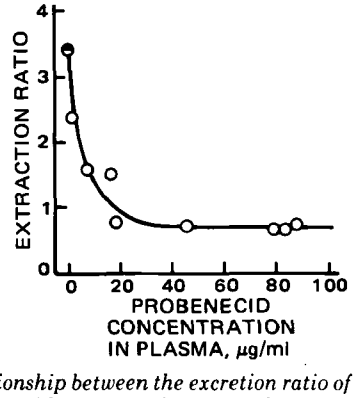


**Figure 4**—*Relationship between the excretion ratio of penicillin G and the plasma probenecid concentration at steady state after the constant and simultaneous infusion of penicillin G, probenecid, and inulin to rats. The point for the control experiment without probenecid (●) represents the mean value (3.41 ± 0.96) of five rats.*

**Metabolic Elimination After Intravenous Bolus Injection**—Paper chromatography of rat urine and bile samples after the intravenous administration of penicillin V detected penicilloic acid ($R_f$ 0.72) and the β-lactam ring-cleaved product of 6-aminopenicillanic acid ($R_f$ 0.35). English *et al.* (23) previously found 6-aminopenicillanic acid as well as penicilloic acid in urine after intravenous and oral administration of some penicillins in animal species. Table II shows that unchanged penicillin V (43%), penicilloic acid (36%), and the sum of 6-aminopenicillanic acid and the β-lactam ring-cleaved product (22%) were excreted over 9 hr both in urine and bile after a single dose of penicillin V. Total recovery in urine and bile was 101 ± 8%. The penicilloic acids were found to be the major metabolites of penicillin G, propicillin, dicloxacillin, and ampicillin (Table III). Kind *et al.* (24) demonstrated that penicillin G and ampicillin were inactivated at different rates by isolated rat liver cells; this suggests a metabolic route for these compounds.

Cafazolin, on the other hand, was recovered almost completely in the intact form in urine and bile after intravenous single-dose administration in rats (Fig. 3). Nishida *et al.* (25) have shown that the amount of recovered cefazolin in 24-hr urine and bile samples were 81 and 17%, respectively, after intramuscular administration to rats. These results show that the metabolism of cefazolin is negligible in rats, similar to other species including the human (5).

**Extraction of Antibiotics from the Circulation by Kidney and**

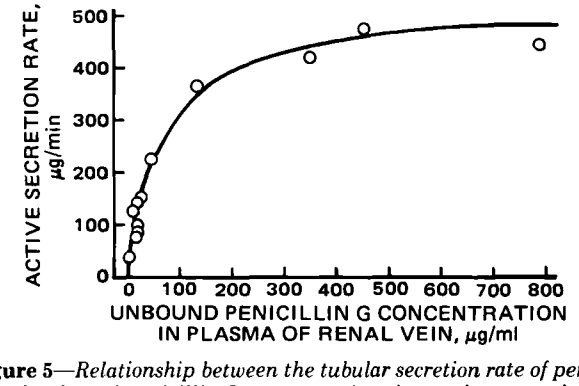


**Figure 5**—*Relationship between the tubular secretion rate of penicillin G and unbound penicillin G concentrations in renal venous plasma at steady state after the constant and simultaneous infusion of penicillin G and inulin to rats. The points represent the experimental values; the solid line was generated from Eq. 5 and the Michaelis–Menten kinetic parameters of Vu = 530.1 μg/min and $K_{m,u}$ = 69.6 μg/ml.*

[21] Lichrosorb Rp-8, 10-μm particle size; E. Merck AG, Darmstadt, W. Germany.
[22] Model TRIROTAR-II; Japan Spectroscopic Co., Tokyo, Japan.
[23] Model UVIDEC 100-III; Japan Spectroscopic Co., Tokyo, Japan.
[24] FACOM M-170F; at the Data Processing Center, Kanazawa University, Kanazawa, Japan.

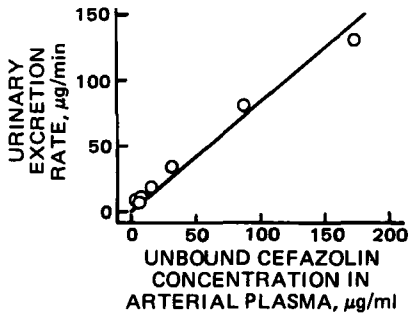


**Figure 6**—*Relationship between the urinary excretion rate of cefazolin and the unbound cefazolin concentration in arterial plasma at steady state after the constant and simultaneous infusion of cefazolin and inulin to rats. The renal clearance was evaluated from the slope of the line drawn through the experimental points.*

**Liver**—*Renal Clearance*—To clarify the renal excretion mechanism of β-lactam antibiotics in rats, the renal clearances of penicillin G and cefazolin were measured. Studies on the relationship between serum protein binding and the renal clearance of drugs are limited. Recently, Levy (26) suggested that the renal tubular secretion rate is a function of the concentration of free drug in the renal venous plasma except for the case of blood flow rate-limited secretion. Hori *et al.* (27) demonstrated that the tubular secretion of sulfathiazole is dependent on the unbound sulfathiazole in plasma. If the renal excretion rate of β-lactam antibiotics is governed by the sum of the rates of glomerular filtration (G) [which is dependent on the unbound antibiotic in the arterial plasma ($C_{F,p}$)] and the capacity-limited tubular secretion (S) [which, in turn, depends on the unbound antibiotic concentration ($C_{F,kd}$) in the renal venous plasma], then the rate expression for urinary excretion may be written as:

$$\frac{dX_u}{dt} = (G + S)(1 - R) \quad \text{(Eq. 3)}$$

$$G = GFR \cdot C_{F,p} \quad \text{(Eq. 4)}$$

$$S = \frac{Vu \cdot C_{F,kd}}{K_{m,u} + C_{F,kd}} \quad \text{(Eq. 5)}$$

where R, $Vu$, and $K_{m,u}$ represent the reabsorption fraction, the maximum rate of tubular secretion, and the Michaelis constant, respectively, and $X_u$ is the amount of antibiotic excreted in the urine.

It was reported that some β-lactam antibiotics are actively secreted into renal tubules in rats, dogs, rabbits, and humans, and that the secretion is completely inhibited by probenecid (4–6). A preliminary experiment was performed to examine the effect of probenecid on the secretion of penicillin G in the rat kidney. The ratio of plasma renal clearance of penicillin G to inulin clearance (the conventional measure of overall renal excretion) was 2.19 ± 0.62 ($n$ = 5) during the control period, where penicillin G was infused at a rate of 12.5 mg/hr. The clearance ratio decreased dramatically (79%) to 0.46 ($n$ = 1) in the period of simultaneous infusion of probenecid at a rate of 2.4 mg/hr. To obtain more precise information for the tubular secretion and reabsorption of penicillins, probenecid was simultaneously infused with penicillin G and inulin to achieve various steady-state probenecid levels. The plots of the steady-state excretion ratio, $(dX_u/dt)_{ss}/G_{ss}$, *versus* the steady-state plasma concentration of probenecid (Fig. 4) show that as the plasma concentration of probenecid increased, the excretion ratio of penicillin G decreased markedly. There was no significant change in the serum protein binding of penicillin G in the presence of probenecid. It is obvious from these results that penicillin G is actively secreted in rats. Since a complete inhibition of the tubular secretion of this antibiotic was attained at >50-μg/ml probenecid levels in plasma, the reabsorption fraction of penicillin G could be obtained from the mean of the data of $(dX_u/dt)_{ss}/G_{ss}$ at >50-μg/ml probenecid levels. This was found to be 0.33 ± 0.03 ($n$ = 4). Decreasing the urine flow by 85% did not significantly change the reabsorption fraction (0.32 ± 0.15, $n$ = 4) of penicillin G in rats, although urine flow rate is known to be one of the factors influencing the tubular reabsorption of drugs (27).

The secretion rate was, therefore, calculated for the data under steady-state conditions and without the administration of probenecid using:

$$S_{ss} = \left(\frac{dX_u}{dt}\right)_{ss}/(1 - R) - GFR(C_{F,p})_{ss} \quad \text{(Eq. 6)}$$

The relationship between the unbound concentration in the renal venous plasma at steady state $(C_{F,kd})_{ss}$ and the steady-state secretion rate $S_{ss}$ of penicillin G (Fig. 5) clearly indicates the saturable secretion of penicillin G. The Michaelis–Menten kinetic parameters for penicillin G tubular secretion, obtained by NONLIN, were $Vu$ = 530.1 ± 49.4 μg/min and $K_{m,u}$ = 69.6 ± 13.8 μg/ml.

Similar experiments were also made for cefazolin. The observed ratio of plasma renal clearance to inulin clearance was 0.35 ± 0.04 ($n$ = 4) in the control period. After probenecid infusion, the value was 0.31 ± 0.03 ($n$ = 4) (probenecid steady-state plasma level of 88 μg/ml), with the differences being statistically insignificant. The results indicate a negligible contribution of the tubular secretion of cefazolin in rats. When the steady-state excretion rates, $(dX_u/dt)_{ss}$, were plotted *versus* the unbound cefazolin concentrations, $(C_{F,p})_{ss}$, there was a linear relationship with a zero intercept and a slope of 0.82 ml/min (Fig. 6). By employing a GFR value of 1.06 ± 0.15 ml/min ($n$ = 4), the R-value for cefazolin was determined to be 0.22. These results demonstrate that cefazolin is excreted mainly by glomerular filtration and then reabsorbed in part by the renal tubules.

*Hepatic Clearance*—Cefazolin was infused into rats with bile fistules to achieve various steady-state plasma levels. Since metabolism of cefazolin was found to be negligible (as described in a previous section), the steady-state biliary secretion rate, $(dX_{bi}/dt)_{ss}$, may be attributed to the uptake of this antibiotic into hepatocytes or biliary secretion itself. If the hepatic uptake is not the rate-limiting step and the biliary secretion rate is capacity limited, the rate can be described by a Michaelis–Menten equation:

$$\left(\frac{dX_{bi}}{dt}\right)_{ss} = \frac{V_{bi}(C_{F,1v})_{ss}}{K_{m,bi} + (C_{F,1v})_{ss}} \quad \text{(Eq. 7)}$$

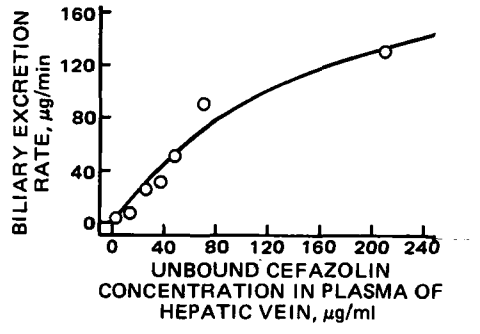


**Figure 7**—*Relationship between the biliary excretion rate of cefazolin and unbound cefazolin concentrations in hepatic venous plasma at steady state after the constant infusion of cefazolin to rats. The points represent the experimental values; the solid line was generated from Eq. 7 and the Michaelis–Menten kinetic parameters of* $V_{bi}$ = 238.8 μg/min *and* $K_{m,bi}$ = 163.3 μg/ml.

**Table IV—Tissue-to-Plasma Partition Coefficients ($Kp$) of β-Lactam Antibiotics for Various Tissues of Rats**

| Tissue | $K_p$[a] Penicillin V | Dicloxacillin | Cefazolin |
|---|---|---|---|
| Lung | 0.157 ± 0.078 ($n$ = 14) | 0.123 ± 0.027 ($n$ = 5) | 0.154 ± 0.078 ($n$ = 8) |
| Heart | 0.095 ± 0.024 ($n$ = 12) | 0.074 ± 0.014 ($n$ = 4) | 0.101 ± 0.022 ($n$ = 15) |
| Muscle | 0.062 ± 0.017 ($n$ = 10) | 0.051 ± 0.014 ($n$ = 4) | 0.077 ± 0.029 ($n$ = 18) |
| Bone | — | — | 0.111 ± 0.021 ($n$ = 15) |
| Skin | — | — | 0.303 ± 0.058 ($n$ = 11) |
| Spleen | 0.096 ± 0.020 ($n$ = 12) | 0.088 ± 0.031 ($n$ = 5) | — |
| Gut | 0.966 ± 0.452 ($n$ = 14) | 1.357 ± 0.590 ($n$ = 12) | 0.114 ± 0.029 ($n$ = 10) |
| Liver | 0.250 ± 0.052 ($n$ = 12)[b] | 0.430 ± 0.287 ($n$ = 9)[c] | 0.788 ± 0.354 ($n$ = 10)[b] |
| Kidney | 3.70 ± 0.87 ($n$ = 14)[b] | 1.27 ± 0.44 ($n$ = 10)[c] | 2.79 ± 1.05 ($n$ = 10)[b] |

[a] The value of $K_p$ is the ratio of tissue concentration to the venous outflow plasma concentration at steady state, as defined by Eq. 8. [b] Corrected by using the corresponding plasma flow rate and the elimination clearance according to the technique described by Chen and Gross (28). [c] Apparent value calculated from the ratio of tissue concentration to the arterial plasma concentration at steady state.

**Table V—*In Vivo* Uptake of β-Lactam Antibiotics into Erythrocytes of Rats**

| β-Lactam Antibiotic | No. of Experiments | Rat Weight, g | $(C_{T,p})_{ss}$,[a] μg/ml | $(C_{WB})_{ss}$,[b] μg/ml | Hematocrit, % | $K_p$[c] |
|---|---|---|---|---|---|---|
| Penicillin G | 4 | 255 ± 5 | 105.9 ± 13.3 | 48.8 ± 5.0 | 54.8 ± 2.1 | 0.016 |
| Penicillin V | 3 | 242 ± 1 | 29.8 ± 4.2 | 12.0 ± 3.2 | 51.3 ± 4.6 | 0 |
| Methicillin | 3 | 254 ± 10 | 63.1 ± 9.0 | 31.2 ± 2.8 | 51.7 ± 2.2 | 0.022 |
| Dicloxacillin | 3 | 241 ± 2 | 36.6 ± 9.4 | 17.4 ± 3.3 | 51.1 ± 3.3 | 0 |
| Ampicillin | 3 | 243 ± 2 | 99.9 ± 14.4 | 44.5 ± 7.4 | 52.2 ± 2.5 | 0 |
| Cephaloridine | 4 | 240 ± 5 | 52.0 ± 8.4 | 26.3 ± 3.2 | 51.5 ± 2.8 | 0.040 |
| Cefazolin | 3 | 238 ± 2 | 77.5 ± 12.3 | 32.9 ± 2.9 | 53.2 ± 3.4 | 0 |

[a] Total antibiotic concentration in arterial plasma at steady state. [b] Total antibiotic concentration in whole blood at steady state. [c] Mean value calculated from Eq. 9. All negative $K_p$ values were listed as zero.

where $V_{bi}$ and $K_{m,bi}$ represent the maximum rate and Michaelis constant, respectively, for the biliary secretion, and $(C_{F,1v})_{ss}$ represents the free antibiotic concentration in hepatic venous plasma at steady state.

Plotting the relationship between $(dX_{bi}/dt)_{ss}$ and $(C_{F,1v})_{ss}$ yielded a convex curvature (Fig. 7). The values of $V_{bi}$ and $K_{m,bi}$ were 238.8 ± 56.8 μg/min and 163.3 ± 65.4 μg/ml, respectively, using NONLIN according to Eq. 7. The magnitudes of the apparent renal clearance of 0.82 ml/min and the biliary secretion parameters of $V_{bi}$ and $K_{m,bi}$ predict that at high cefazolin free levels, urinary excretion is superior to biliary secretion, and at low levels both excretions may be comparable.

**Tissue-to-Plasma Partition Coefficient**—The steady-state tissue-to-plasma concentration ratios, $K_p$, of penicillin V, dicloxacillin, and *cefazolin were measured* experimentally for each rat tissue compartment (Table IV). The $K_p$ for any organ is defined by:

$$K_{p,i} = \frac{(C_{T,i})_{ss}}{(C_{F,i} + C_{B,i})_{ss}} \quad \text{(Eq. 8)}$$

where $(C_{T,i})_{ss}$ and $(C_{F,i} + C_{B,i})_{ss}$ represent the total antibiotic concentration in a whole tissue (excluding blood) and total antibiotic concentration in the tissue venous plasma, respectively, at steady state. For noneliminating organs, the steady-state arterial plasma concentration, $(C_{T,p})_{ss}$, was used for the calculation as $(C_{T,p})_{ss} = (C_{F,i} + C_{B,i})_{ss}$. When an antibiotic concentration in the venous plasma of kidney or liver was not measured, the $K_p$ value was corrected by using the corresponding plasma flow rate and clearance, as suggested by Chen and Gross (28).

The $K_p$ values of β-lactam antibiotics in all tissues except gut and kidney were found to be <1. The antibiotics studied were highly concentrated in the kidney, which is the major eliminating organ. Penicillin V and dicloxacillin exhibited extremely higher $K_p$ values in gut tissue than cefazolin. This phenomenon may be the result of an extensive contribution of enterohepatic recirculation of the former two antibiotics (12). Because of the almost negligible intestinal absorption of cefazolin in rats (29), cefazolin provided the true $K_p$ value for gut tissue.

Distribution of several β-lactam antibiotics into erythrocytes was evaluated by measuring the steady-state concentrations in whole blood and plasma of rats. The $K_p$ value for erythrocytes was calculated from:

$$K_p = 1 + \left[\frac{(C_{WB})_{ss}}{(C_{T,p})_{ss}} - 1\right] \Big/ (\text{Hct}/100) \quad \text{(Eq. 9)}$$

where $(C_{WB})_{ss}$ is the whole blood concentration at steady state. The results (Table V) indicate negligible distribution of β-lactam antibiotics into the rat erythrocyte compartment. Nishida *et al.* (30) previously demonstrated that distribution of penicillins into rabbit erythrocytes was <3% or negligible after intravenous bolus administration; their results are consistent with our observations.

**Development of the Physiologically Based Pharmacokinetic Model**—Figure 8 is a diagrammatic representation of a noneliminating organ subdivided anatomically into three fluid compartments: (*a*) the capillary blood volume, (*b*) the interstitial fluid, and (*c*) the intracellular space. In formulating the kinetics of β-lactam antibiotics in these tissues (except the liver and kidney), the following assumptions, based on the experimental evidence described in the previous and subsequent sections, were made.

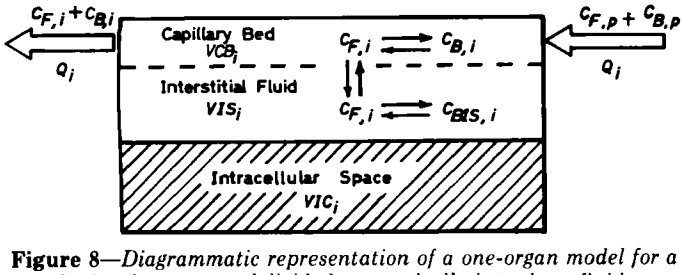


**Figure 8**—*Diagrammatic representation of a one-organ model for a noneliminating organ subdivided anatomically into three fluid compartments.*

1. Free and bound antibiotics entering with arterial plasma mix with the antibiotics in the tissue capillary bed.
2. Only the mixed antibiotics in the capillary bed, which is free from plasma protein binding, can diffuse rapidly in the tissue (except bone).
3. Entrance into the intracellular space by the antibiotic is negligible; therefore, the diffused antibiotic is restricted to the interstitial fluid of the tissue.
4. The antibiotic diffused into the interstitial fluid can bind only with albumin existing in this compartment, in a similar manner as with plasma albumin.
5. Bone tissue is divided into three compartments consisting of capillary bed, bone marrow, and bone cortex. The bone marrow-to-plasma ratio is assumed to be 1. The antibiotic binds in the bone marrow exactly as in the plasma, and only unbound antibiotics can diffuse into the bone cortex fluid space.
6. A well-mixed state exists in the capillary bed, interstitial fluid, and bone regions.
7. Free and bound antibiotic concentrations in venous plasma leaving the tissues are the same as those in the capillary bed.

From the above assumptions regarding the distribution of β-lactam antibiotics in noneliminating organs (except bone), a mass balance equation can be expressed as:

$$VCB_i\left(\frac{dC_{F,i}}{dt} + \frac{dC_{B,i}}{dt}\right) + VIS_i\left(\frac{dC_{F,i}}{dt} + \frac{dC_{BIS,i}}{dt}\right) = Q_i(C_{F,p} + C_{B,p}) - Q_i(C_{F,i} + C_{B,i}) \quad \text{(Eq. 10)}$$

The nomenclature for this equation and others is given in Appendix I (Glossary). The two terms of the left-hand side of Eq. 10 represent the accumulation rates of free and bound antibiotics in the capillary bed and interstitial fluid, respectively. Differentiation of the plasma binding equations (Eqs. 1 and 2) yields:

$$\frac{dC_{B,i}}{dt} = \alpha_i \frac{dC_{F,i}}{dt} \quad \text{(Eq. 11)}$$

In the case of nonlinear binding behavior:

$$\alpha_i = \frac{nPK_B}{(1 + K_B C_{F,i})^2} \quad \text{(Eq. 12)}$$

Similarly, linear binding yields:

$$\alpha_i = K_{B,app}P \quad \text{(Eq. 13)}$$

Taking the tissue-to-plasma albumin concentration ratio, $AR_i$, for *i*-type tissue and using assumption 4, Eq. 10 can be simplified to:

$$[VCB_i(1 + \alpha_i) + VIS_i(1 + \alpha_i AR_i)]\frac{dC_{F,i}}{dt} = Q_i[(1 + \beta_p)C_{F,p} - (1 + \beta_i)C_{F,i}] \quad \text{(Eq. 14)}$$

where $\beta_i$ can be defined for the nonlinear binding case as:

$$\beta_i = \frac{nPK_B}{1 + K_B C_{F,i}} \quad \text{(Eq. 15)}$$

and in the linear binding case, $\beta_i = \alpha_i$. If assumption 5 is valid, the mass

**Table VI—Hepatic Blood Flow by a Continuous Indocyanine Green Infusion Method in Anesthetized Rats [a]**

| Anesthesia | No. of Experiments | Body Weight, g | Liver Weight, g | Hematocrit, % | $Q_{p,1v}$[b]/100 g body, ml/min | $Q_{p,1v}$[b]/liver, ml/min | $Q_{b,1v}$[c]/100 g body, ml/min | $Q_{b,1v}$[c]/liver, ml/min |
|---|---|---|---|---|---|---|---|---|
| Urethane | 4 | 245 ± 7 | 7.4 ± 0.6 | 52.0 ± 3.9 | 1.52 ± 0.29 | 0.50 ± 0.10 | 3.17 ± 0.66 | 1.04 ± 0.23 |
| Ether | 3 | 246 ± 2 | 7.3 ± 0.1 | 46.0 ± 1.0 | 2.24 ± 1.10 | 0.75 ± 0.36 | 4.15 ± 2.04 | 1.39 ± 0.67 |
| Ether[d] | 5 | 308 ± 8 | 11.7 ± 1.7 | 41.0 ± 5.0 | 1.99 ± 0.46 | 0.53 ± 0.11 | 3.38 ± 0.73 | 0.90 ± 0.17 |
| Control[d] | 4 | 312 ± 8 | 12.3 ± 1.6 | 39.0 ± 4.0 | 3.69 ± 0.51 | 0.93 ± 0.07 | 6.05 ± 0.74 | 1.53 ± 0.06 |

[a] Each point represents the mean ± *SD*. [b] Hepatic plasma flow. [c] Hepatic blood flow which was calculated from: $Q_{b,1v} = Q_{p,1v}/(1 - \text{Hematocrit}/100)$. [d] Data taken from Yokota *et al.* (15).

balance in the bone compartment can be written as Eq. II-5 (Appendix II).

In the mathematical description for the eliminating organs such as the liver and kidney, $K_p$ values were employed to predict the tissue concentrations, because uptake and accumulation of antibiotics into the intracellular spaces appeared to be difficult to evaluate at the present time. Okada *et al.* (31) demonstrated recently that the extent of binding of cefazolin, cephaloridine, cephalexin, and cloxacillin with 90% of liver and kidney homogenates was 2~65% for rats and beagle dogs, and that the tissue binding appears to be unrelated to the binding of the drugs to serum albumin. β-Lactam antibiotics are highly protein-bound with the water-soluble hepatic and renal intracellular protein, ligandin (32). The binding between the drugs and ligandin may correlate with their hepatic and renal uptakes from plasma.

A full diagram of blood circulation through various tissues is represented in Fig. 9. All pertinent tissues for which antibiotic concentrations are known, except for carcass (fat and others), have been included. The plasma flow of the liver (Table VI) and the tissue volumes of the heart, liver, and kidney used for the calculations were experimental values determined in this laboratory. The organ flow rates, except for the liver, and volumes of the other tissues were taken from published physiological values (8, 10, 33–35), adjusted to reflect the size of the animals studied. Sapirstein *et al.* (34) determined that in rats, bronchial blood flow constituted only 3% of cardiac output. Based on this simulation study, the contribution of the bronchial circulation to antibiotic distribution into lung tissue was assumed to be negligible. The physiological parameters employed in this study are listed in Table VII.

*Binding to the Interstitial Protein*—If assumptions 2 and 3 are valid for β-lactam antibiotics in noneliminating organs (except bone), the following mass balance equation can be written:

$$C_{T,i} = IS_i(C_{F,i} + C_{BIS,i}) \qquad \text{(Eq. 16)}$$

where IS is the interstitial space expressed by:

$$IS_i = \frac{VIS_i}{VIS_i + VIC_i} \qquad \text{(Eq. 17)}$$

From assumption 3, for the antibiotics showing nonlinear serum protein binding behavior, Eq. 1 can be written as:

$$C_{BIS,i} = \frac{n \cdot AR_i \cdot PK_B C_{F,i}}{1 + K_B C_{F,i}} \qquad \text{(Eq. 18)}$$

Since $C_{F,i} = C_{F,p}$ in noneliminating organ regions, except bone, at steady state, Eqs. 16 and 18 can be expressed as:

$$(C_{T,i})_{ss} = IS_i \cdot \left[1 + \frac{n \cdot AR_i \cdot PK_B}{1 + K_B(C_{F,p})_{ss}}\right](C_{F,p})_{ss} \qquad \text{(Eq. 19)}$$

Similarly in the case of linear binding:

$$(C_{T,i})_{ss} = IS_i \cdot (1 + AR_i \cdot PK_{B,app})(C_{F,p})_{ss} \qquad \text{(Eq. 20)}$$

The interstitial space ($IS_i$) of lung, heart, skin, bone, gut, and liver in rats was estimated from the distribution of inulin or [$^{14}$C]inulin. The value of $IS_i$ for each tissue was calculated as the ratio of tissue to plasma concentrations at steady state (Table VIII). The interstitial water content of most tissues was 10–20%. The IS value of skin, however, was 30% of the blood-free organ, much higher than that found in the other tissues studied. Our results were consistent with those reported by Higaki and Fujimoto (36) using data after intravenous bolus injection of [$^{14}$C]inulin in kidney-ligated rats, but were less than IS values evaluated (37) from the mannitol and thiosulfate spaces. The reason for larger spaces determined by the latter two compounds may be due to their partial distribution into the intracellular compartment.

Cefazolin seems to be a good model to test the validity of Eq. 19 or 20, because of its remarkable nonlinear binding characteristics with rat albumin. Figure 10 illustrates plots of the steady-state tissue concentration $(C_{T,i})_{ss}$ *versus* the steady-state arterial plasma free concentration $(C_{F,p})_{ss}$ obtained for heart, muscle, skin, and gut.

When we used the $AR_i$ values of 0.5, 0.6, and 0.9 reported (37) for heart, muscle, and gut, respectively, the curves generated from Eq. 19 using the binding parameters of cefazolin listed in Table I and the corresponding interstitial space in Table VIII were in good agreement with the experimental tissue levels of cefazolin. Katz *et al.* (37) demonstrated that AR values for muscle and skin were ~0.55, but the interstitial albumin content of skin and gut was twice that of muscle in rats. Rothschild *et al.* (38) found that most of the extravascular albumin was located in the skin in humans, and the concentration of albumin in the extravascular and extracellular skin approaches that in the plasma. The high level of albumin in skin is likely to be related to the high interstitial space of this tissue (Table VIII). The observed skin levels fit well with the curves generated from Eq. 19 with the reasonable assumption of AR = 1. Figure 10 clearly indicates that the free concentration of cefazolin in plasma at <20 μg/ml had a greater effect on the tissue levels than did cefazolin plasma concentrations >50 μg/ml. This is a result of the nonlinear binding with rat plasma albumin and is described by Eq. 19.

Little basic information has been reported concerning antibiotic concentrations in bone, especially bone marrow. Pitkin *et al.* (39) found that cefazolin levels were detected in bone and bone marrow of normal rabbits dosed intramuscularly even in the absence of detectable levels in serum. However, the concentration ratio of bone cortex to bone marrow of this antibiotic was ~0.05 (39). More recently, it was found (40) that the concentrations of cefazolin in bone marrow were equal to or exceeded that in serum 60 min after the administration of 50 mg/kg iv in rabbits. Because bone marrow sampling was difficult in rats, we used a beagle dog to evaluate assumption 5. The results (Table IX) indicate that the observed cefazolin levels in whole bone marrow, although somewhat scattered, were almost equal to the whole blood levels at steady state. Since the mean whole blood levels were well described using Eq. 9 with the mean steady-state plasma levels and hematocrit of 41% (assuming $K_p$

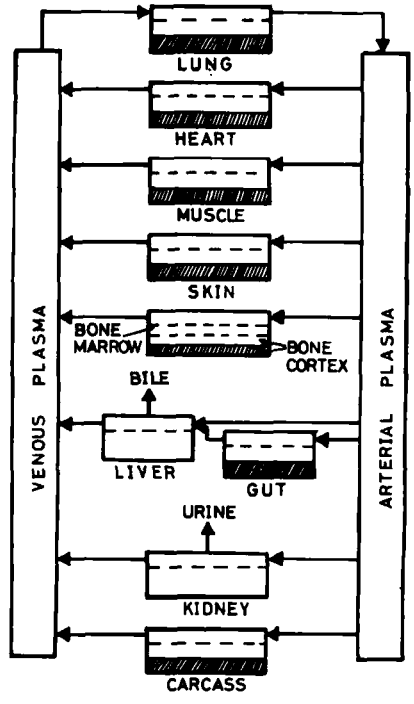


**Figure 9**—*Physiological pharmacokinetic model fully diagramming the blood circulation through various tissues.*

**Table VII—Physiological Parameters for 240-g Rats [a]**

| Tissue | Total Tissue Volume ($V$), ml | Interstitial Fluid Volume ($VIS$)[b], ml | Plasma Volume in Capillary Bed ($VCB$)[c], ml | Plasma Flow Rate ($Q$), ml/min | Tissue-to-Plasma Albumin Ratio (AR) |
|---|---|---|---|---|---|
| Venous blood pool | 2.9 | — | 1.4[d] | 30.0 | 1.0 |
| Arterial blood pool | 1.5 | — | 0.8[d] | 30.0 | 1.0 |
| Lung | 1.6 | 0.3 | 0.3 | 30.0 | 0.5 |
| Heart | 1.0[e] | 0.1 | 0.2 | 0.8 | 0.5 |
| Muscle | 108.0 | 13.0 | 0.7 | 3.6 | 0.6 |
| Skin | 43.0 | 13.0 | 0.2 | 2.4 | 1.0 |
| Bone | 26.0 | 3.0 | 1.1[f] | 0.8 | 1.0[g] |
| Gut | 16.0 | 1.5 | 3.0 | 2.6 | 0.9 |
| Liver | 8.0[e] | 1.3 | 1.0 | 3.7 | 0.5 |
| Kidney | 2.0[e] | 0.4 | 2.5 | 7.3 | 0.5 |
| Carcass (fat, others) | 14.0 | 2.0 | 0.1 | 11.4 | 0.5 |

[a] Based on the values in Refs. 8, 10, 33–35, and 37. [b] Calculated from the equation: $VIS = V \times$ (Inulin space). The inulin spaces for various tissues except kidney and carcass are listed in Table VIII. For kidney tissue, the inulin space of 19.6% is reported in Ref. 36. For carcass, 15% inulin space was assumed. [c] Estimated from the values reported in Refs. 10 and 56 under the assumption that rats, dogs, and humans have the same ratio of blood volume in capillary bed-to-tissue volume without blood. [d] 50% hematocrit was assumed. [e] Determined experimentally in this laboratory. [f] Including bone marrow. [g] Bone marrow.

= 0), it is safe to conclude that the bone marrow-to-plasma concentration ratio was almost unity, consistent with previous observations in humans (41, 42).

The validity of Eq. 19 or 20 was also tested by comparing the $K_p$ values observed for dicloxacillin and penicillin V as well as cefazolin (Table IV) and those calculated by combining Eqs. 1, 8, and 19:

$$(K_{p,i})_{calc} = IS_i \frac{1 + K_B(C_{F,p})_{ss} + n \cdot AR_i \cdot PK_B}{1 + K_B(C_{F,p})_{ss} + nPK_B} \quad \text{(Eq. 21)}$$

or Eqs. 2, 18, and 20:

$$(K_{p,i})_{calc} = IS_i \frac{1 + AR_i \cdot PK_{B,app}}{1 + PK_{B,app}} \quad \text{(Eq. 22)}$$

For bone tissue, Eq. 21 may be rewritten using assumption 5 for the nonlinear binding case:

$$(K_{p,bn})_{calc} = \frac{IS_{bn}[1 + K_B(C_{F,p})_{ss}] + S_{bnm}nPK_B}{1 + K_B(C_{F,p})_{ss} + nPK_B} \quad \text{(Eq. 23)}$$

where $IS_{bn}$ and $S_{bnm}$ represent inulin space and bone marrow space, respectively, in bone tissue. The AR values of lung and $S_{bnm}$ were assumed to be 0.5 and 0.038 (Table VII), respectively; the binding parameters were taken from Table I. There is a good agreement between observed (Table IV) and calculated $K_p$ values in all cases (Fig. 11), indicating that assumptions 3–5 made for tissue distribution of β-lactam antibiotics are reasonable and applicable, at least for noneliminating organs.

*Application to Tissue Distribution Kinetics of Inulin*—Prior to testing the validity of the physiologically based pharmacokinetic model developed for the body distribution of β-lactam antibiotics, the model was used to simulate the tissue distribution kinetics of inulin in rats. Since inulin is known to be excreted almost completely by glomerular filtration and its distribution is restricted only to plasma and tissue interstitial fluid, the present model has an intrinsic ability to predict the concentration–time profiles of inulin in any tissue.

In the adaptation of this model to a compound having a large molecular size such as inulin, however, the capillary wall permeability must be handled somewhat differently. The capillary walls in lung, heart, muscle, skin, and gut are composed of an interlocking mosaic of endothelial cells with slits (43). Therefore, the restricted transport of inulin through the capillary walls in these tissues does not allow the instantaneous establishment of the equilibrium of inulin between the capillary bed and interstitial fluid. Such a restricted transport of inulin has been apparently described by Fick's law of diffusion (43c–45). The mass balance equations for lung, muscle, skin, and gut tissues are shown in Appendix III. By using values of 20 ml/min/100 g of tissue for lung and heart, 10 ml/min/100 g of tissue for gut, and 2 ml/min/100 g of tissue for muscle and skin as the permeability constants $K_i$ (44, 45); 1.20 ml/min as the GFR (determined for 240-g rats from repeated experimental trials in our laboratory); and the tissue volumes and plasma flows listed in Table VII, the 16 differential equations were solved numerically by a digital computer. The results of the simulations are shown in Figs. 12 and 13. The predicted curves, except for muscle, are in good agreement with the mean values of the experimentally determined tissue levels of inulin after a 20-mg/kg dose and the plasma levels after both 20- and 200-mg/kg iv doses. The predicted peak inulin concentrations for the poorly perfused muscle and skin are reached relatively late, *i.e.*, 10–15 min after the bolus administration. However, the experimental concentration–time profiles in muscle and skin did not show such slow appearance of inulin. This may be the result of a more rapid uptake of inulin into the muscle and skin interstitial fluids from the capillary walls in rats than that reported for rabbits and dogs (44).

*Application to Tissue Distribution Kinetics of Cefazolin*—The differential equations described for cefazolin in Appendix II were solved numerically by incorporating various constants listed in Tables I, IV, and VII. Figures 14 and 15 show the predicted and observed concentration profiles for plasma, lung, heart, muscle, skin, bone, liver, and kidney tissues after the intravenous bolus injection of cefazolin to the urethane-anesthetized rats. Figure 16 also compares the simulation results from the model and the experimental tissue levels of plasma, muscle, skin, and kidney 60 min after the administration of cefazolin at various doses. As seen in these figures, there was reasonable agreement between the model predictions and the experimental concentrations in plasma and in various tissues at any time after any dose.

The physiological parameters in Table VII are statistical average values, and the plasma flow rates (except for liver) are those under unanesthetized conditions. It is, therefore, necessary to test the stability of the present model by comparing the numerical results derived from standard values for all parameters with the numerical results derived

**Table VIII—[$^{14}$C]Inulin Space of Various Tissue of Rats**

| Tissue | Steady-State Concentration, μg/ml or μg/g | | | | | | Inulin Space[a], % |
|---|---|---|---|---|---|---|---|
| | Experiment 1 | Experiment 2 | Experiment 3 | | | | |
| Plasma | 13.6 ± 0.2 | 16.4 ± 0.7 | 20.5 ± 1.6 | | | | 100.0 |
| Heart | 1.77 | 2.05 | 2.36 | | | | 12.3 ± 0.8 |
| Muscle | 1.94 | 1.46 | 2.58 | | | | 11.9 ± 2.8 |
| Skin | 4.07 | 4.50 | 6.66 | | | | 29.9 ± 2.6 |
| Bone | 2.14 | 2.42 | 3.13 | | | | 15.2 ± 0.5 |
| Gut | 1.35 | 1.70 | 1.65 | | | | 9.6 ± 1.2 |
| Liver | 2.37 | 2.87 | 3.22 | | | | 16.9 ± 1.0 |
| | Experiment 4 | Experiment 5 | Experiment 6 | Experiment 7 | Experiment 8 | Experiment 9 | |
| Plasma[b] | 220.6 | 256.6 | 288.0 | 383.8 | 463.6 | 499.0 | 100.0 |
| Lung[b] | 43.1 | 49.6 | 64.8 | 78.3 | 96.4 | 99.8 | 20.4 ± 1.2 |

[a] Defined by 100 × ratio of tissue-to-plasma concentration at steady state. [b] Experiments without [$^{14}$C]inulin. Inulin concentrations in plasma and the lung tissue were determined by a colorimetric assay described in the text.

Table IX—Cefazolin Concentrations in Plasma, Whole Blood, and Whole Bone Marrow After Constant Infusion [a] of Cefazolin in a 9-kg Beagle Dog

| | Concentration, μg/ml | | | | | | | | | | | | |
|---|---|---|---|---|---|---|---|---|---|---|---|---|---|
| | Time, min | | | | | | | | | | | | |
| | 380 | 385 | 410 | 415 | 420 | 450 | 470 | 477 | 483 | 500 | 507 | 517 | Mean ± *SD* |
| Plasma | 67.6 | — | 54.5 | — | 53.3 | 74.8 | 82.2 | — | 95.6 | 65.3 | — | 60.0 | 69.2 ± 14.5 |
| Whole blood | — | — | — | — | 44.9 | 45.5 | — | — | 41.3 | — | — | 39.1 | 42.7 ± 3.0 |
| Whole bone marrow | — | 27.9 | — | 57.7 | — | — | — | 41.5 | — | — | 61.5 | — | 47.2 ± 15.5 |
| Hematocrit, % | — | — | — | — | 41.0 | 41.6 | — | — | 42.5 | — | — | 42.1 | 41.8 ± 0.6 |

[a] Infusion was carried out at a rate of 180 mg/hr without a priming dose.

from ±10% variation of standard values for each of the parameters. Such variation in any body region of the tissue, capillary volumes, and plasma flow rates did not significantly affect the simulation results, indicating that the model is quite stable within ±10% of the physiological parameters.

## DISCUSSION

The binding of antimicrobial agents to plasma protein and tissues is considered to be an important factor in antimicrobial activity and pharmacokinetics. Much of the research effort has been directed toward determining the binding to plasma protein, uptake by erythrocytes, and the extravascular binding of β-lactam antibiotics. Nevertheless, the data are still incomplete in certain aspects: the published reports are sometimes in conflict. This study investigates the full disposition characteristics of β-lactam antibiotics in rats and describes a pharmacokinetic model that is capable of predicting tissue distribution and elimination kinetics not only in rats, but also in other species including humans.

β-Lactam antibiotics bind to serum protein, mainly albumin, in a reversible manner (46). It is generally accepted that such a binding equilibrium occurs within microseconds. Greene *et al.* (47) confirmed the rapid binding of cefazolin to canine serum, the binding equilibrium being attained as fast as the sample could be ultrafiltered. There is a general lack of agreement in the literature regarding the extent of binding for β-lactam antibiotics obtained from experiments carried out by different methods and even by the same method. The equilibrium dialysis method is known to be very reliable for determining quantitative binding of stable drugs, but has disadvantages for unstable drugs due to the time requirement to complete the diffusion equilibrium processes. However, use of microdiffusion cells in this study achieved the complete diffusion equilibrium within 4 hr (Fig. 1).

The serum protein binding ratio of β-lactam antibiotics varies with the species of animal and the total concentration of antibiotic. Shimizu (48) compared the protein binding of penicillins and cephalosporins in the sera of different animals using centrifugal ultrafiltration techniques. The extent of binding of cefazolin was ≥90% in humans, rabbits, and rats (equivalent to that of dicloxacillin), but only ~50% in dogs, horses, and bovines. The percent of cefazolin bound to human serum albumin significantly decreased with increases in the total antibiotic concentration (48). Similar results were obtained in this study using rat serum. The free fraction of cefazolin is 11% at 10 μg/ml, 20% at 100 μg/ml, and 41% at 200 μg/ml. Since the free fraction more than doubled between 10 and 100 μg/ml and increased by a factor of >4 between 10 and 200 μg/ml, the

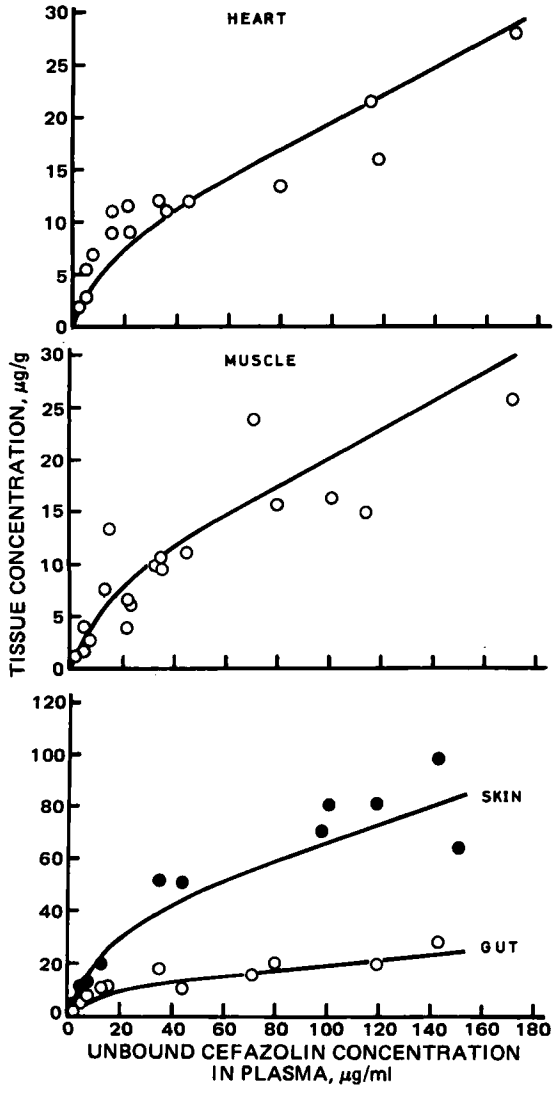


**Figure 10**—*Relationship between cefazolin concentration in the heart, muscle, skin, and gut tissues and the unbound cefazolin concentration in plasma at steady state after the constant infusion of cefazolin to rats. The points represent the experimental values; the solid lines were generated from Eq. 19 and the various parameters listed in Tables I, VII, and VIII.*

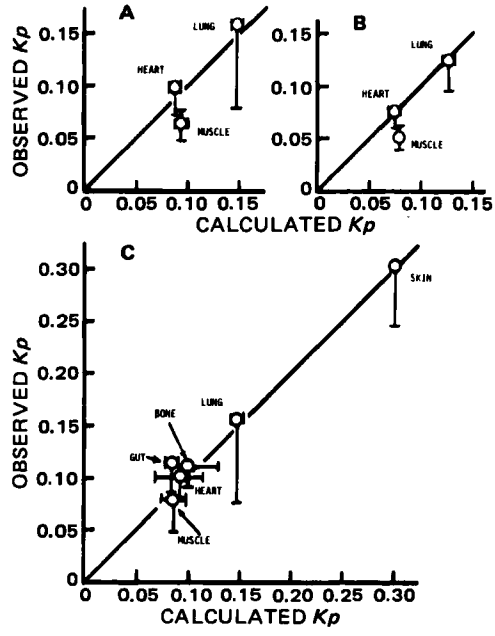


**Figure 11**—*Relationship between the observed $K_p$ values of penicillin V (A), dicloxacillin (B), and cefazolin (C) for various tissues and the theoretical $K_p$ values calculated from Eq. 21 or 23 and the various parameters listed in Tables I, VII, and VIII. The bars represent the standard deviation of the experimental values and the lower and upper limits of the theoretical values.*

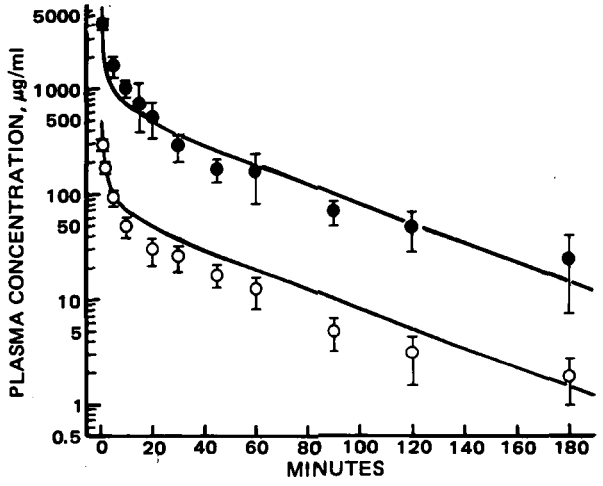


**Figure 12**—*Model-predicted (lines)* versus *observed (points) plasma inulin concentrations after 20- (○) and 200-mg/kg (●) intravenous bolus doses to rats. Each point represents the mean of 3–8 rats; bars represent the standard deviations.*

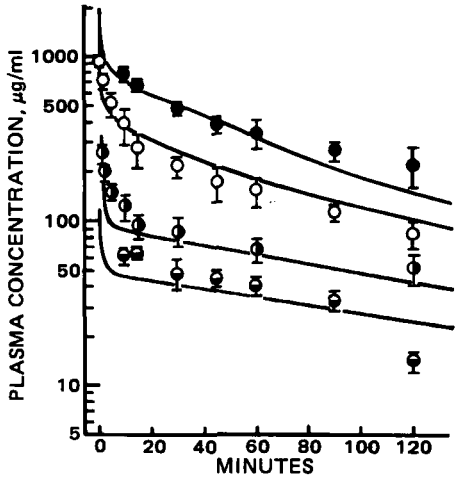


**Figure 14**—*Model-predicted (lines)* versus *observed (points) plasma cefazolin concentrations after 10- (◒), 20- (◑), 100- (○), and 200-mg/kg (●) intravenous bolus doses to rats. Each point represents the mean of 3–9 rats; bars represent the standard deviations.*

distribution of cefazolin into tissue regions in rats will change radically. Other β-lactam antibiotics studied did not show such a remarkable nonlinear binding behavior.

The binding behavior of β-lactam antibiotics could be explained by the nonlinear binding equation (Eq. 1), where the magnitude of the binding constant ($K_B$) and the drug concentration ($C_F$) are very important parameters. If $K_B$ is sufficiently small, Eq. 1 becomes Eq. 2, which expresses an apparent linear binding. Nayler (49) reported that the apparent binding constant of penicillins in human serum correlated quantitatively with the lipophilicity of the antibiotics. The experimental results shown in Fig. 2 and Table I demonstrate that the extent of binding of the five penicillins studied in rat serum correlates qualitatively with their lipophilicity. Dicloxacillin, which is the most lipophilic, has the largest $K_{B,app}$ value, whereas the more hydrophilic methicillin has a smaller $K_{B,app}$ value.

The mechanism of hepatic elimination of β-lactam antibiotics is not clearly understood. Although the penicillin derivatives studied were subjected to extensive metabolism to the penicilloic acids (4), cefazolin did not exhibit such metabolism in rats. The reason for the resistance of cefazolin to metabolic degradation is not clear, but similar results have been reported in other species including humans (5, 6).

The processes concerned with the transport of drugs into bile have been studied (50). Although passive diffusion may play a part in the transport of drug into bile, it is generally believed that active transport is the primary process (50). The biliary secretion of some penicillins and cephalosporins in rats have been studied by Ryrfeldt (51) and Wright and Line

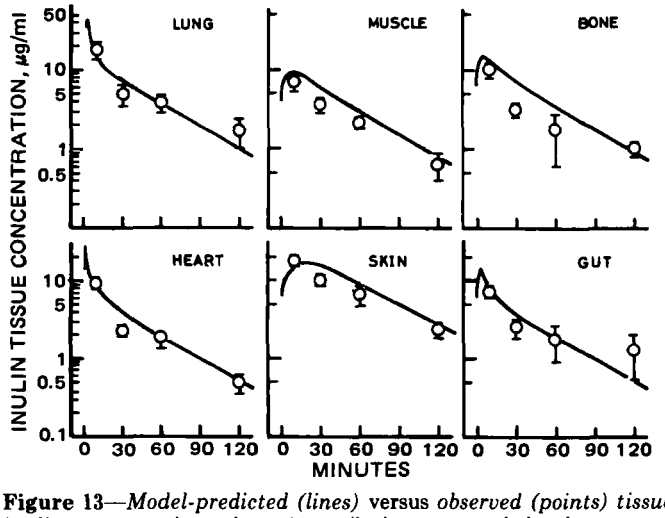


**Figure 13**—*Model-predicted (lines)* versus *observed (points) tissue inulin concentrations after a 20-mg/kg intravenous bolus dose to rats. Each point represents the mean of 3–5 rats; bars represent the standard deviations.*

(52). However, quantitative reports on the biliary excretion rate are limited. Previously, the biliary excretion of penicillin V was characterized by Michaelis–Menten kinetics (12). A similar capacity-limited excretion into bile was also observed for cefazolin, using Eq. 7.

The renal excretion of β-lactam antibiotics has been studied extensively. Using the micropuncture technique, Bergeron *et al.* (53) reported that penicillin G was excreted from plasma by glomerular filtration and active secretion from the proximal tubules, and that the respective contribution ratios were ~35 and 65%. The present study utilizing the net inhibitory effect of probenecid on the renal excretion of penicillin G into rat urine showed 35% glomerular filtration and 65% tubular secretion, consistent with the result of Bergeron *et al.* (53). On the other hand, the rate of cefazolin excretion into urine was unaffected by probenecid. The results indicate that the renal tubular secretion of cefazolin plays a minor role in the renal elimination process in rats. Our conclusion obtained for this antibiotic does not agree with the recent finding by Yamazaki *et al.* (54), who predicted a significant contribution of tubular secretion of cefazolin in rats. This apparent discrepancy cannot be explained completely by the difference in the protein binding ratio determined in both laboratories and needs to be investigated further. Therefore, until such time when a reliable urinary excretion mechanism of β-lactam antibiotics is established, we adopted the apparent renal clearance value of 0.82 ml/min (dependent on the unbound concentration in the arterial plasma) in this pharmacokinetic prediction for cefazolin in rats.

The kinetic behavior of antibiotics in an infected tissue fluid is important for antimicrobial chemotherapy. Classical approaches are usually based on the curve-fitting of plasma concentration data with multiexponential equations to construct the necessary compartment models. Sometimes, the compartments and parameters thus estimated have no physiological reality in the species being investigated. Therefore, it is difficult to use classical pharmacokinetics to interpret the differences between animal and human experiments.

To overcome this difficulty, physiological pharmacokinetic models have been developed and adapted for some drugs by several workers (7–12). These models are based on experimental data regarding tissue binding or tissue-to-plasma (or blood) partition coefficients ($K_p$) in laboratory animals, as with penicillin V (12). This approach has the potential advantages of predicting tissue drug levels and reflecting the variations in drug binding with different tissues of the animals investigated. However, because there are sometimes substantial differences in $K_p$ values among species (11) and the property of $K_p$ in each tissue is often obscure, this approach does not always allow us to predict the tissue concentration–time profiles of drugs in other species, *i.e.*, humans.

Our present goal was to make possible *a priori* predictions of β-lactam antibiotic levels in organs of any species, based on the knowledge of parameters easily determined for human subjects as well as experimental animals. This study was designed to use cefazolin, which exhibits interesting nonlinear binding with serum proteins and simpler elimination characteristics in rats than the other β-lactam antibiotics.

One of the key points in solving this problem is to clarify the exact nature of the $K_p$ values of β-lactam antibiotics for various tissues. Peterson *et al.* (55) determined the binding of some β-lactam antibiotics

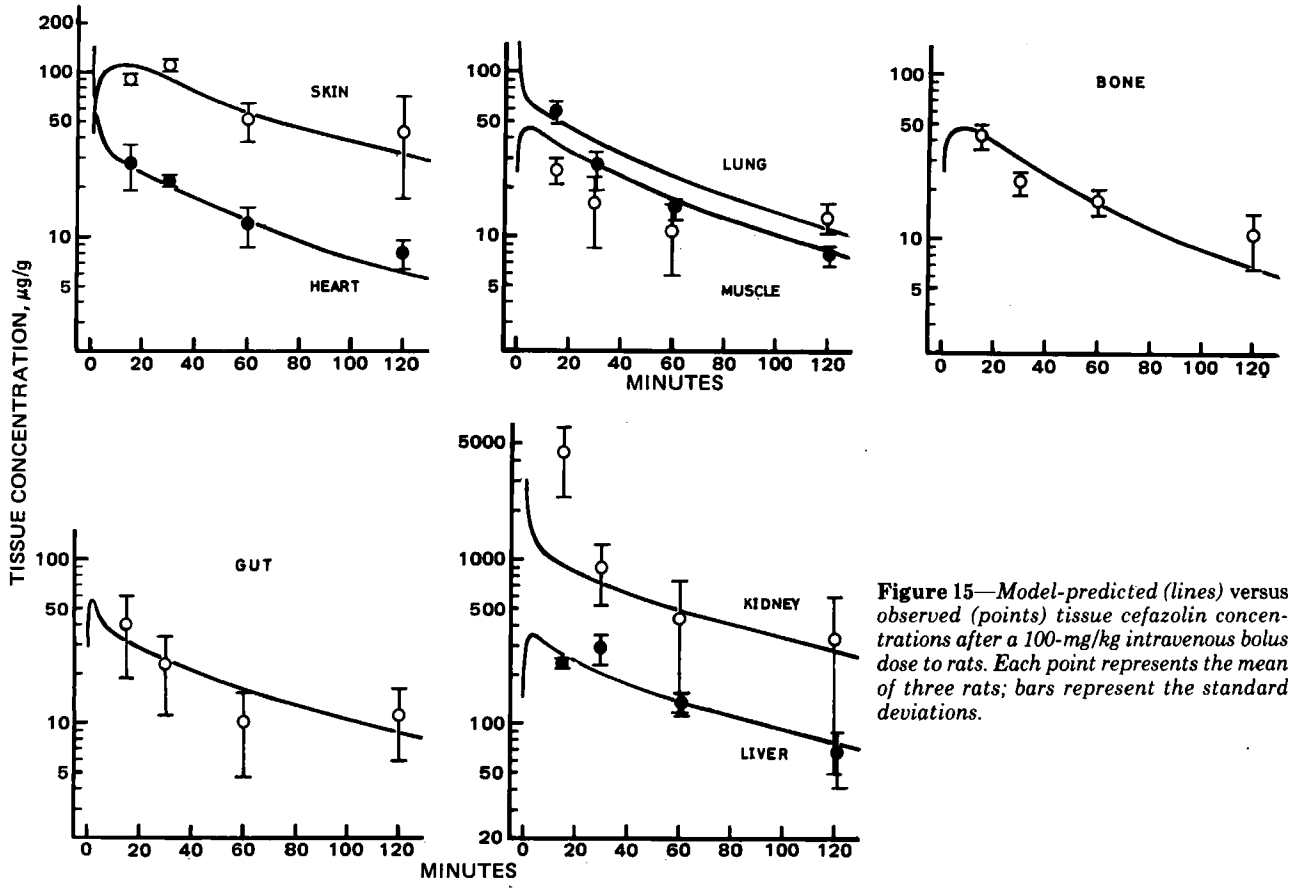


**Figure 15**—*Model-predicted (lines)* versus *observed (points) tissue cefazolin concentrations after a 100-mg/kg intravenous bolus dose to rats. Each point represents the mean of three rats; bars represent the standard deviations.*

in dilute homogenates of canine tissues and employed the results to predict the apparent volume of distribution after intravenous administration in dogs. The question may be raised whether binding data obtained *in vitro* with tissue homogenates are applicable to *in vivo* conditions. For a drug that is unable to penetrate into the tissue intracellular space, binding to tissue apparently was not the sole factor responsible for *in vivo* accumulation of the drug. With β-lactam antibiotics, however, due to the experimental difficulty in assessing the extent of antibiotic penetration into cells, the conclusions obtained from the various animal model studies differed among investigators. By determining the steady-state plasma and tissue levels of cefazolin in rats, we obtained evidence in support of our claim that this antibiotic cannot enter erythrocytes and tissue cells of noneliminating organs, and that albumin existing in these tissue interstitial fluids play a major role in determining antibiotic levels in various tissues. On this basis, the $K_p$ values of β-lactam antibiotics could be successfully interpreted for not only cefazolin, but also penicillin V and dicloxacillin.

Despite the use of simplifying assumptions in formulating the antibiotic distribution in physiologically and anatomically complex body regions, there was a reasonably close fit between the simulation from the present model and the experimental tissue levels after intravenous bolus administration of cefazolin in rats. The simulations demonstrate that the tissue distribution of cefazolin in rats is complete within 15 min even in the slowly perfused muscle, skin, and bone tissues. The observed high cefazolin level in skin compared with the levels in the other noneliminating tissues is due to the higher content of albumin and the larger interstitial space. The time course of cefazolin in skin was also nicely predicted by the present pharmacokinetic model based on the assumption that albumin concentration in the skin interstitial fluid is equal to that in plasma. In addition to the examination for β-lactam antibiotics, this model could predict the tissue distribution profiles of inulin. The model, incorporating the slow diffusion of a large molecule from capillary membranes into the interstitial fluids of lung, heart, muscle, skin, and gut tissues, was able to adequately represent the concentrations of inulin in plasma and various tissues. As seen in Fig. 13, inulin in skin showed a markedly different behavior from cefazolin, and the concentration–time profile in skin was almost identical with those in heart, muscle, bone, and gut; this is the consequence of the lack of binding of inulin with albumin. This result supports the assumption made for the skin compartment in the present work.

Although our model was able to provide a good prediction of intravenous dosing data of cefazolin and inulin in rats, there are still a number of deficiencies. First, it is necessary to identify the magnitude of uptake clearance of antibiotics into hepatocytes compared with hepatic plasma flow rate. Second, we need to more fully characterize the kinetics and mechanisms not only of active transport into tubular cells and reabsorption from tubules in the kidney, but also biliary secretion and metabolism in the liver for the β-lactam antibiotics. The proposed model, nevertheless, is capable of predicting tissue concentrations as a function of time after a single bolus dose in normal animals and should be useful in predicting these levels in animals where renal and hepatic function, albumin concentration, extravascular space, and blood flow are altered due to disease states.

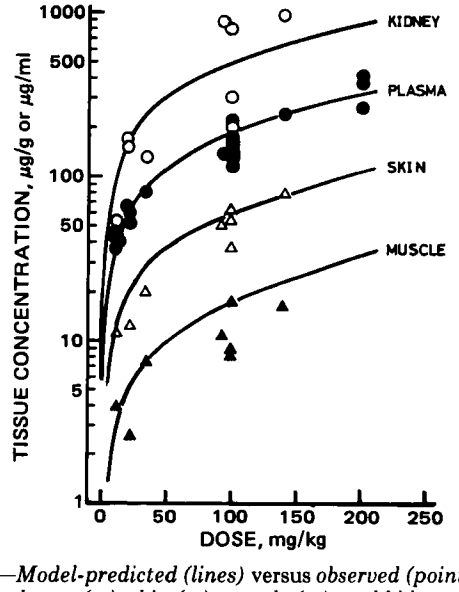


**Figure 16**—*Model-predicted (lines)* versus *observed (points) concentrations in plasma (●), skin (△), muscle (▲), and kidney (○) 60 min after intravenous bolus injections at various doses to rats.*

## APPENDIX I: GLOSSARY

AR = Tissue-to-plasma albumin ratio
$C_B$ = Bound concentration in plasma, μg/ml
$C_{BIS}$ = Bound concentration in tissue interstitial fluid, μg/ml
$C_F$ = Free concentration in plasma or in tissue interstitial fluid, μg/ml
$C_T$ = Total concentration in tissue, μg/ml or μg/g
GFR = Glomerular filtration rate, ml/min
$I(t)$ = Dose input function, $min^{-1}$
IS = Tissue interstitial space
$K$ = Permeability constant from capillary wall to interstitial fluid, ml/min
$K_m$ = Michaelis constant, μg/ml
$K_p$ = Tissue-to-plasma partition coefficient
$P$ = Albumin concentration in serum, $M$
$Q$ = Plasma flow rate, ml/min
R = Reabsorption ratio
UF = Urine flow rate, ml/min
$V$ = Volume of tissue (excluding equilibrium blood), ml
$\nabla_{bi}$ = Maximum rate of biliary secretion, μg/min
VCB = Plasma volume in capillary bed of tissue, ml
VIC = Volume of tissue intracellular water, ml
VIS = Volume of tissue interstitial fluid, ml
$\alpha$ = Coefficient in the differentiation of the plasma protein binding
$\beta$ = *Bound-to-unbound* concentration ratio

Subscripts
b = blood
p = arterial plasma
u = urine
bi = bile
vp = venous plasma
lg = lung
lgi = lung interstitial fluid
ht = heart
hti = heart interstitial fluid
ms = muscle
msi = muscle interstitial fluid
sk = skin
ski = skin interstitial fluid
bn = bone
bnm = bone marrow
bnc = bone cortex
gt = gut
gti = gut interstitial fluid
cr = carcass
lv = liver
kd = kidney
wb = whole blood
ss = steady state

## APPENDIX II: MODEL EQUATIONS FOR CEFAZOLIN

**Venous plasma:**

$$V_{vp}(1+\alpha_{vp})\frac{dC_{F,vp}}{dt} = Q_{ht}(1+\beta_{ht})C_{F,ht} + Q_{ms}(1+\beta_{ms})C_{F,ms} + Q_{sk}(1+\beta_{sk})C_{F,sk} + Q_{bn}(1+\beta_{bn})C_{F,bn} + Q_{cr}(1+\beta_{cr})C_{F,cr} + Q_{lv}(1+\beta_{lv})C_{F,lv} + Q_{kd}(1+\beta_{kd})C_{F,kd} - (Q_{ht}+Q_{ms}+Q_{sk}+Q_{bn}+Q_{cr}+Q_{lv}+Q_{kd})(1+\beta_{vp})C_{F,vp} + \text{Dose}\cdot I(t) \quad \text{(Eq. II-1)}$$

**Arterial plasma:**

$$V_p(1+\alpha_p)\frac{dC_{F,p}}{dt} = (Q_{ht}+Q_{ms}+Q_{sk}+Q_{bn}+Q_{cr}+Q_{lv}+Q_{kd}) \times [(1+\beta_{lg})C_{F,lg} - (1+\beta_p)C_{F,p}] \quad \text{(Eq. II-2)}$$

**Lung:**

$$[VCB_{lg}(1+\alpha_{lg}) + VIS_{lg}(1+\alpha_{lg}AR_{lg})]\frac{dC_{F,lg}}{dt} = (Q_{ht}+Q_{ms}+Q_{sk}+Q_{bn}+Q_{cr}+Q_{lv}+Q_{kd})[(1+\beta_{vp})C_{F,vp} - (1+\beta_{lg})C_{F,lg}] \quad \text{(Eq. II-3)}$$

**Heart:**

$$[VCB_{ht}(1+\alpha_{ht}) + VIS_{ht}(1+\alpha_{ht}AR_{ht})]\frac{dC_{F,ht}}{dt} = Q_{ht}[(1+\beta_p)C_{F,p} - (1+\beta_{ht})C_{F,ht}] \quad \text{(Eq. II-4)}$$

**Muscle:**

$$[VCB_{ms}(1+\alpha_{ms}) + VIS_{ms}(1+\alpha_{ms}AR_{ms})]\frac{dC_{F,ms}}{dt} = Q_{ms}[(1+\beta_p)C_{F,p} - (1+\beta_{ms})C_{F,ms}] \quad \text{(Eq. II-5)}$$

**Skin:**

$$[VCB_{sk}(1+\alpha_{sk}) + VIS_{sk}(1+\alpha_{sk}AR_{sk})]\frac{dC_{F,sk}}{dt} = Q_{sk}[(1+\beta_p)C_{F,p} - (1+\beta_{sk})C_{F,sk}] \quad \text{(Eq. II-6)}$$

**Bone:**

$$[(VCB_{bn}+V_{bnm})(1+\alpha_{bn}) + VIS_{bnc}]\frac{dC_{F,bn}}{dt} = Q_{bn}[(1+\beta_p)C_{F,p} - (1+\beta_{bn})C_{F,bn}] \quad \text{(Eq. II-7)}$$

**Carcass:**

$$[VCB_{cr}(1+\alpha_{cr}) + VIS_{cr}(1+\alpha_{cr}AR_{cr})]\frac{dC_{F,cr}}{dt} = Q_{cr}[(1+\beta_p)C_{F,p} - (1+\beta_{cr})C_{F,cr}] \quad \text{(Eq. II-8)}$$

**Liver:**

$$[(1+\alpha_{lv})(VCB_{lv}+V_{lv}K_{p,lv})]\frac{dC_{F,lv}}{dt} = (Q_{lv}-Q_{gt})(1+\beta_p)C_{F,p} + Q_{gt}(1+\beta_{gt})C_{F,gt} - Q_{lv}(1+\beta_{lv})C_{F,lv} - \frac{V_{biCF,lv}}{K_{m,bi}+C_{F,lv}} \quad \text{(Eq. II-9)}$$

**Gut tissue:**

$$[VCB_{gt}(1+\alpha_{gt}) + VIS_{gt}(1+\alpha_{gt}AR_{gt})]\frac{dC_{F,gt}}{dt} = Q_{gt}[(1+\beta_p)C_{F,p} - (1+\beta_{gt})C_{F,gt}] \quad \text{(Eq. II-10)}$$

**Kidney:**

$$[(1+\alpha_{kd})(VCB_{kd}+V_{kd}K_{p,kd})]\frac{dC_{F,kd}}{dt} = Q_{kd}[(1+\beta_p)C_{F,p} - (1+\beta_{kd})C_{F,kd}] - GFR(1-R)C_{F,p} \quad \text{(Eq. II-11)}$$

where the dose input function can be calculated as the function of the reciprocal of the injection time, λ (7):

$$I(t) = 30\lambda(\lambda t)^2(1-\lambda t)^2 \quad \text{(Eq. II-12)}$$

The values of $\alpha_i$ and $\beta_i$ are defined by Eqs. 12 and 15, respectively, in the text.

Total concentration in plasma and total tissue concentration corresponding to the observed values in $i$-type tissue, except liver and kidney, can be calculated from Eqs. II-13 and II-14, respectively:

$$C_{T,p} = (1+\beta_p)C_{F,p} \quad \text{(Eq. II-13)}$$

$$C_{T,i} = IS_i(1+\beta_i AR_i)C_{F,i} \quad \text{(Eq. II-14)}$$

Calculation of total tissue concentration in liver and kidney is made from:

$$C_{T,i} = (1+\beta_i)K_{pi}C_{F,i} \quad (i = \text{liver, kidney}) \quad \text{(Eq. II-15)}$$

## APPENDIX III: MODEL EQUATIONS FOR INULIN

Instead of Eqs. II-3 to II-6 and II-10 in Appendix II, the following mass balance equations can be written for the lung, heart, muscle, skin, and gut regions (see text).

**Lung:**

$$VCB_{lg}\frac{dC_{F,lg}}{dt} = Q_{lg}(C_{F,pv} - C_{F,lg}) - K_{lg}(C_{F,lg} - C_{F,lgi}) \quad \text{(Eq. III-1)}$$

$$VIS_{lg}\frac{dC_{F,lgi}}{dt} = K_{lg}(C_{F,lg} - C_{F,lgi}) \qquad \text{(Eq. III-2)}$$

**Heart:**

$$VCB_{ht}\frac{dC_{F,ht}}{dt} = Q_{ht}(C_{F,p} - C_{F,ht}) - K_{ht}(C_{F,ht} - C_{F,hti}) \qquad \text{(Eq. III-3)}$$

$$VIS_{ht}\frac{dC_{F,hti}}{dt} = K_{ht}(C_{F,ht} - C_{F,hti}) \qquad \text{(Eq. III-4)}$$

**Muscle:**

$$VCB_{ms}\frac{dC_{F,ms}}{dt} = Q_{ms}(C_{F,p} - C_{F,ms}) - K_{ms}(C_{F,ms} - C_{F,msi}) \qquad \text{(Eq. III-5)}$$

$$VIS_{ms}\frac{dC_{F,msi}}{dt} = K_{ms}(C_{F,ms} - C_{F,msi}) \qquad \text{(Eq. III-6)}$$

**Skin:**

$$VCB_{sk}\frac{dC_{F,sk}}{dt} = Q_{sk}(C_{F,p} - C_{F,sk}) - K_{sk}(C_{F,sk} - C_{F,ski}) \qquad \text{(Eq. III-7)}$$

$$VIS_{sk}\frac{dC_{F,ski}}{dt} = K_{sk}(C_{F,sk} - C_{F,ski}) \qquad \text{(Eq. III-8)}$$

**Gut:**

$$VCB_{gt}\frac{dC_{F,gt}}{dt} = Q_{gt}(C_{F,p} - C_{F,gt}) - K_{gt}(C_{F,gt} - C_{F,gti}) \qquad \text{(Eq. III-9)}$$

$$VIS_{gt}\frac{dC_{F,gti}}{dt} = K_{gt}(C_{F,gt} - C_{F,gti}) \qquad \text{(Eq. III-10)}$$

Elimination of inulin was negligible in the liver and occurs in the kidney through glomerular filtration, where negligible reabsorption (R = 0) can be assumed. Because there is no binding of inulin with any protein, $\alpha_i = 0$ and $\beta_i = 0$, then $C_{T,i} = IS_iC_{F,i}$ in every tissue region.

## REFERENCES


(1) M. Gibaldi, M. A. Schwartz, and M. E. Plaut, *Antimicrob. Agents Chemother.—1968*, **1969**, 378.

(2) L. W. Dittert, W. O. Griffen, Jr., J. C. LaPiana, F. J. Shaifeld, and J. T. Doluisio, *Antimicrob. Agents Chemother.—1969*, **1970**, 42.

(3) R. E. Notari, "Biopharmaceutics and Pharmacokinetics, an Introduction," 2nd ed., Dekker, New York, N.Y., 1975, (References cited therein).

(4) T. Bergan, *Antibiot. Chemother.*, **25**, 1 (1978) (References cited therein).

(5) C. H. Nightingale, D. S. Greene, and R. Quintiliani, *J. Pharm. Sci.*, **64**, 1899 (1975) (References cited therein).

(6) J. M. Brogard, F. Comte, and M. Pinget, *Antibiot. Chemother.*, **25**, 123 (1978) (References cited therein).

(7) K. B. Bischoff and R. L. Dedrick, *J. Pharm. Sci.*, **57**, 1346 (1968).

(8) K. B. Bischoff, R. L. Dedrick, D. S. Zaharko, and J. A. Longstreth, *J. Pharm. Sci.*, **60**, 1128 (1971).

(9) N. Benowitz, R. P. Forsyth, K. L. Melmon, and M. Rowland, *Clin. Pharmacol. Ther.*, **16**, 87 (1974).

(10) C. N. Chen and J. D. Andrade, *J. Pharm. Sci.*, **65**, 717 (1976).

(11) L. I. Harrison and M. Gibaldi, *J. Pharm. Sci.*, **66**, 1679 (1977).

(12) A. Tsuji, E. Miyamoto, T. Terasaki, and T. Yamana, *J. Pharm. Pharmacol.*, **31**, 116 (1979).

(13) D. S. Greene, R. Quintiliani, and C. H. Nightingale, *J. Pharm. Sci.*, **67**, 191 (1978).

(14) M. A. Schwartz and A. J. Delduce, *J. Pharm. Sci.*, **58**, 1137 (1969).

(15) M. Yokota, T. Iga, S. Awazu, and M. Hamano, *J. Appl. Physiol.*, **41**, 439 (1976).

(16) S. E. Bradley, F. J. Ingelfinger, G. P. Bradley, and J. J. Curry, *J. Clin. Invest.*, **24**, 890 (1945).

(17) R. Thomas, *Nature (London)*, **191**, 1161 (1961).

(18) A. Tsuji, E. Miyamoto, and T. Yamana, *J. Pharm. Pharmacol.*, **30**, 811 (1978).

(19) K. Miyazaki, O. Ogino, and T. Arita, *Chem. Pharm. Bull.* **12**, 413 (1964).

(20) W. H. Waugh, *Clin. Chem.*, **23**, 639 (1977).

(21) R. K. Harle and T. Cowen, *Analyst*, **103**, 492 (1978).

(22) C. M. Metzler, "NONLIN, A Computer Program for Parameter Estimation in Nonlinear Systems," Technical Report 7292/69/7292/005, The Upjohn Co., Kalamazoo, Mich., 1969.

(23) A. R. English, H. T. Huang, and B. A. Sobin, *Proc. Soc. Exp. Biol. Med.*, **104**, 405 (1960).

(24) A. C. Kind, H. N. Beaty, L. F. Fenster, and W. M. M. Kirby, *J. Lab. Clin. Med.*, **71**, 728 (1968).

(25) M. Nishida, T. Matsubara, T. Murakawa, Y. Mine, Y. Yokota, S. Goto, and S. Kuwahara, *J. Antibiot.*, **23**, 184 (1970).

(26) G. Levy, *J. Pharm. Sci.*, **69**, 482 (1980).

(27) (*a*) R. Hori, K. Sunayashiki, and A. Kamiya, *J. Pharm. Sci.*, **65**, 463 (1976); (*b*) R. Hori, K. Sunayashiki, and A. Kamiya, *Chem. Pharm. Bull.*, **26**, 740 (1978) (References cited therein).

(28) H. S. G. Chen and J. F. Gross, *J. Pharmacokinet. Biopharm.*, **7**, 117 (1979).

(29) A. Tsuji, E. Miyamoto, O. Kubo, and T. Yamana, *J. Pharm. Sci.*, **68**, 812 (1979).

(30) M. Nishida, T. Matsubara, T. Uemura, T. Murakawa, and Y. Yokota, *Jpn. J. Antibiot.*, **23**, 217 (1970).

(31) N. Okada, H. Sakamoto, S. Nakamoto, Y. Yokota, T. Murakawa, and M. Nishida, *Chemotherapy (Tokyo)*, **25**, 392 (1977).

(32) (*a*) M. L. Kornguth, R. A. Monson, and C. M. Kunin, *J. Infect. Dis.*, **129**, 552 (1974); (*b*) R. Kirsch, G. Fleischner, K. Kamisaka, and I. M. Arias, *J. Clin. Invest.*, **55**, 1009 (1975).

(33) L. Jansky and J. S. Hart, *Can. J. Physiol. Pharmacol.*, **46**, 653 (1968).

(34) L. A. Sapirstein, E. H. Sapirstein, and A. Bredemeyer, *Circ. Res.*, **8**, 135 (1960).

(35) R. L. Dedrick, D. S. Zaharko, and R. J. Lutz, *J. Pharm. Sci.*, **62**, 882 (1973).

(36) K. Higaki and M. Fujimoto, *J. Physiol. Soc. Jpn.*, **31**, 164 (1969).

(37) J. Katz, G. Bonorris, S. Golden, and A. L. Sellers, *Clin. Sci.*, **39**, 705 (1970).

(38) M. A. Rothschild, A. Bauman, R. S. Yalow, and S. A. Berson, *J. Clin. Invest.*, **34**, 1334 (1955).

(39) D. H. Pitkin, C. Sachs, I. Zajac, and P. Actor, *Antimicrob. Agents Chemother.*, **11**, 760 (1977).

(40) E. Dingeldein and H. Wahlig, *Arzneim.-Forsch, Drug Res.*, **29**, 400 (1979).

(41) T. Shidou, *Jpn. J. Antibiot.*, **29**, 999 (1976).

(42) M. Kawashima and T. Torisu, *Jpn. J. Antibiot.*, **30**, 278 (1977).

(43) (*a*) G. Majino, in "Handbook of Physiology," Sect. 2, vol. III, W. F. Hamilton and P. Dow, Eds., American Physiological Society, Washington, D.C., 1963, p. 1035; (*b*) J. G. Luft, in "The Inflammatory Process," B. W. Zweifach, L. Grant, and R. T. McCluskey, Eds., Academic, New York, N.Y., 1965, p. 121; (*c*) E. M. Penkin, *Circ. Res.*, **41**, 735 (1977).

(44) L. E. Wittners, Jr., M. Bartlett, and J. A. Johnson, *Microvas. Res.*, **11**, 67 (1976).

(45) (*a*) W. P. Paaske and P. Sejrsen, *Acta Physiol. Scand.*, **100**, 437 (1977); (*b*) W. P. Paaske, *Physiologist*, **23**, 75 (1980).

(46) G. N. Rolinson and R. Sutherland, *Brit. J. Pharmacol.*, **25**, 638 (1965).

(47) D. S. Greene, R. Quintiliani, and C. H. Nightingale, *J. Pharm. Sci.*, **66**, 1663 (1977).

(48) T. Shimizu, *Jpn. J. Antibiot.*, **27**, 296 (1974).

(49) J. H. C. Nayler, in "Advances in Drug Research," vol. 7, N. J. Harper and A. B. Simmonds, Eds., Academic, New York, N.Y., 1973, p. 1.

(50) C. T. Ashworth and E. Sanders, *Am. J. Pathol.*, **37**, 343 (1960).

(51) A. Ryrfeldt, *Acta Pharmacol. Toxicol.*, **32**, Suppl., III, 1 (1973).

(52) W. E. Wright and V. D. Line, *Antimicrob. Agents Chemother.*, **17**, 842 (1980).

(53) M. G. Bergeron, F. J. Gennari, M. Barza, L. Weistein, and S. Cortell, *J. Infect. Dis.*, **132**, 374 (1975).

(54) I. Yamazaki, Y. Shirakawa, and T. Fugono, *J. Antibiot.*, **34**, 1055 (1981).

(55) L. R. Peterson, D. N. Gerding, D. McLinn, and W. H. Hall, *J. Antimicrob. Chemother.*, **5**, 219 (1979).

(56) W. W. Mapleson, *J. Appl. Physiol.*, **18**, 197 (1963).

ACKNOWLEDGMENTS

Presented in part at the 12th Symposium on Drug Metabolism and Action, Kanazawa, Japan, Oct. 8–9, 1980.

The authors are indebted to Dr. Shinobu Nakamura, School of Medicine, Kanazawa University, for the bone marrow sampling and helpful discussions. Thanks are also given to Mr. H. Nakamura, Miss Y. Yoshida, Miss K. Narizuka, Miss H. Hironaka, Miss M. Nishikawa, Miss M. Uwagawa, and Mr. H. Mizuo for their excellent assistance in the experimental work and to Fujisawa Pharmaceutical Co., Osaka, Japan for the supply of [$^{14}$C]cefazolin.

# Solution Activity Product ($K_{FAP}$) and Simultaneous Demineralization–Remineralization in Bovine Tooth Enamel and Hydroxyapatite Pellets

**JEFFREY L. FOX *‡¶ˣ, BALA V. IYER *‡, WILLIAM I. HIGUCHI *‡¶, and JOHN J. HEFFERREN §**

Received May 17, 1982, from the **Dental Research Institute* and the ‡*College of Pharmacy, The University of Michigan, Ann Arbor, MI 48109* and the §*American Dental Association Health Foundation.* Accepted for publication August 26, 1982. ¶Present address: Dept. of Pharmaceutics, University of Utah, Salt Lake City, UT 84112.

**Abstract** □ The effects of changing the ion activity product of the remineralization solution at pH 4.5 ($pK_{FAP}$ 108–118) on the remineralization behavior of demineralized bovine tooth enamel and hydroxyapatite pellets have been studied. Solutions containing calcium-45, phosphate, and fluoride in acetate buffers were used. The $^{45}$Ca/F molar ratios indicated the formation of fluoridated hydroxyapatite in the enamel or the pellet when the $pK_{FAP}$ values for remineralizing solutions were <112. When the $pK_{FAP}$ values were >112, the $^{45}$Ca/F ratios were found to be ≪5. Also, when the $pK_{FAP}$ values were large (>112), the remineralization patterns based on the fluoride distribution in the tooth (or pellet) were found to be different than when the $pK_{FAP}$ values were small (<112). The hypothesis that a $pK_{FAP}$ value of 112 is the demarcation between remineralization only and simultaneous dissolution–remineralization has been proposed based on these results.

**Keyphrases** □ Tooth enamel—bovine, demineralization and remineralization, effect of bulk solution activity product □ Hydroxyapatite—pellets, demineralization and remineralization, effect of bulk solution activity product □ Remineralization—demineralized bovine tooth enamel, hydroxyapatite pellets, effect of bulk solution activity product

Previous studies conducted in these laboratories (1) indicated that both bovine tooth enamel and hydroxyapatite pellets could be extensively remineralized in a fluoride-containing remineralizing solution after prior demineralization treatments for various lengths of time. After 3 or 6 hr of prior demineralization in a partially saturated acetate buffer at pH 4.5, fluoride uptake levels on the order of 1000 ppm were found after remineralization, at depths up to ~50 μm from the surface. The stoichiometry of the remineralized phase was shown to be fluoridated hydroxyapatite rather than calcium fluoride based on the $^{45}$Ca/F ratio and determination by X-ray diffraction analysis. All of the remineralization studies (1) were conducted in solutions at an ionic product ($K_{FAP} = a^{10}_{Ca^{2+}} a^{6}_{PO_4^{3-}} a^{2}_{F^-}$) of $\sim 1 \times 10^{-108}$.

The purpose of the present study was to investigate the influence of varying the $K_{FAP}$ value for the remineralizing solution. A case of special interest was where the $K_{FAP}$ values are $>10^{-120}$, the solubility product for fluorapatite (2), but $<10^{-114}$, the ion activity product value below which dissolution takes place with hydroxyapatite pellets (3). A question of great interest was how the concomittant dissolution of hydroxyapatite, if it were to occur, would influence the remineralization behavior in this $K_{FAP}$ region.

## EXPERIMENTAL

**Materials**—*Bovine Teeth*—Teeth from 8-week-old strictly kosher calves were obtained from packing houses in the Chicago area. From these incisors, only those without any visible surface defects and with a reasonably flat surface were used for the experiments. The labial surfaces of these selected teeth were then ground with rotating sandpaper (No. 400 first, then No. 600) to remove the pellicle.

*Hydroxyapatite Pellet*—Synthetic hydroxyapatite crystals prepared using the procedure developed by Moreno (4) were used in the preparation of the pellets. Approximately 50 mg of hydroxyapatite, preequilibrated in a humidity chamber containing saturated potassium nitrate aqueous solution to maintain the humidity at ~67%, was compressed in a 0.62-cm diameter die with a force of 4540 kg using a laboratory press[1].

*Preparation of Buffer Solutions*—As in a previous study (1) a solution ~16% saturated (on a molar basis) with respect to the thermodynamic solubility of hydroxyapatite was used for demineralization. The solution was a 0.1 *M* acetate buffer containing 3.5 m*M* each of total calcium and phosphate. The pH was adjusted to 4.5 with sodium hydroxide and the ionic strength to 0.5 *M* by the addition of sodium chloride. For remineralization 0.1 *M* acetate buffers (pH 4.5) containing differing amounts of total calcium and phosphate depending on the desired bulk solution activity product ($K_{FAP} = a^{10}_{Ca^{2+}} a^{6}_{PO_4^{3-}} a^{2}_{F^-}$) as shown in Table I, were employed. These solutions also contained 10 ppm of fluoride and sodium chloride to adjust the ionic strength to 0.5 *M*. All the chemicals used for the preparation of buffer solutions were analytical grade. A predetermined amount of calcium-45 as $^{45}CaCl_2$ in water[2] was added to these solutions.

**Demineralization**—A bovine tooth was covered with dental inlay wax except for a 0.25-cm$^2$ area in the labial surface. In the pellet experiments, a hydroxyapatite pellet was completely covered with inlay wax except for one exposed surface (area, 0.25 cm$^2$). The tooth or pellet was then demineralized in the 16% partially saturated buffer solution for a period of 6 and 3 hr, respectively, after attaching a thin glass rod to each (length, ~14 cm). The glass rod was used to ensure careful handling during demineralization and remineralization. The use of 6 and 3 hr as the demineralization times was based on previous experimental results (1) which clearly indicated that the demineralizing solution was not saturated

[1] Carver Press.
[2] New England Nuclear, Boston, Mass.



*0022-3549/83/1100-1252$01.00/0*